

AN INVESTIGATION OF THE PYROXENITE MARKER AND THE ASSOCIATED  
ROCKS IN THE MAIN ZONE OF THE EASTERN BUSHVELD COMPLEX

by

CONSTANCE LOUGENE MARAIS

Submitted in partial fulfilment of the requirements  
for the degree of Master of Science, in the faculty  
of Science, University of Pretoria

PRETORIA

OCTOBER 1977

Optical investigation of the orthopyroxenes also revealed a compositional break in the differentiation sequence at the height of the Pyroxenite Marker. A reversal in the trend of iron enrichment is recorded at all four of the localities examined. At the same stratigraphic height the orthopyroxene is poorer in iron in the north than in the south. The compositional trends of the plagioclase from the four localities resemble those of the orthopyroxene.

Separated pyroxenes were analysed chemically by means of the energy dispersive analyses of x-rays (EDAX) method. Whole-rock samples were also analysed by means of EDAX.

Quantitative trace-element analyses on the whole rock and on separated cumulus minerals were carried out by atomic absorption spectrometry (AAS) for the elements barium, chromium, cobalt, copper, nickel, strontium and zinc, whereas ion exchange chromatography was used for titanium and vanadium. Variation in the chromium and nickel contents with fractionation was shown to conform with that predicted by crystal field theory. At the Pyroxenite Marker the reversal of the normal fractionation trend is borne out by the partitioning of chromium.

The reversed fractionation trend, as well as the partitioning of the trace elements at the level of the Pyroxenite Marker, are inconsistent with the process of continuous fractionation within the magma chamber. The gradual addition of undifferentiated magma during crystallization of the upper part of Subzone B,

followed by a larger, sudden influx of magma at the level of the Pyroxenite Marker, were probably responsible for the observed relationships.

## SAMEVATTING

Hierdie studie behels 'n mineralogiese, petrografiese en spoorelementondersoek van die gesteentes wat voorkom bokant en onderkant die Piroksenietmerker van die Hoofsone van die Bosveldkompleks in die Oos-Transvaal.

Ontledings is gedoen van monsters versamel langs roetes op Thornhill 544KS in Sekhukhuneland, by Roossenekal en op Galgstroom (Mapochsgronde 500JS) en op Tonteldoos (Mapochsgronde 500JS) oos van Stoffberg, asook van monsters verkry van 'n boorkern afkomstig van Steelpoortpark 366KT noord van Roossenekal. Die Piroksenietmerker is nie by Tonteldoos ontwikkel nie, maar 'n klinopirokseennorietlaag bo 'n fynkorrelrige, magnetietryke ortopirokseengabbro word beskou om dieselfde horison te wees.

Modale ontledings van slypplaatjies van die vier gebiede toon dat die fynkorrelrige gesteentes 'n hoër magnetietinhoud in die suide as in die noorde het. Dit kom voor asof die uitkristallisering van magnetiet tot gevolg gehad het dat voldoende FeO vanuit die magma ontrek is om 'n afname in oplosbaarheid van swael, en die gevolglike vorming van 'n onmengbare sulfiedvloeistof te veroorsaak. Die laer temperatuur in die suide het ook die uitwerking gehad dat die oplosbaarheid van die swael in die magma verminder is.

Geïnverteerde pigeoniet is die Ca-arm pirokseen in Subsone B van die Hoofsone, maar dit verander skielik na

primêre ortopirokseer by die basis van die Piroksenietmerker van Subsone C.

Optiese bepalings van die samestelling van die ortopiroksene het ook 'n onderbreking in die differensiasieverloop op die hoogte van die Piroksenietmerker aan die lig gebring. 'n Omkering in die ysterverryking word waargeneem in al vier gebiede waar die ondersoek gedoen is. Op dieselfde stratigrafiese hoogte is die ortopirokseer armer aan yster in die noorde as in die suide. Die verandering in die samestelling van die plagioklaas afkomstig van die vier gebiede toon dieselfde neigings as dié van die ortopirokseer.

Die piroksene is chemies ontleed deur middel van die EDAX-metode (energy dispersive analyses of x-rays). Monsters van die gesteentes is ook deur middel van EDAX ontleed.

Kwantitatiewe ontledings van spoorelemente is uitgevoer op die geheelgesteentes asook op die kumulusminerale deur middel van atoomabsorpsiespektrometrie (AAS). Dié metode is gevolg vir die elemente barium, chroom, kobalt, koper, nikkel, stronsium en sink. Ioonuitruilingschromatografie is egter gebruik vir titaan en vanadium. Variasie in chroom- en nikkelinhoud met fraksionasie het geblyk in ooreenstemming te wees met die kristalveldteorie. By die Piroksenietmerker word die omkering van die normale fraksionasietendens aangedui deur die verspreiding van chroom.

Die omgekeerde verloop van fraksionasie, asook die verspreiding van die spoorelemente op die vlak van die Piroksenietmerker is nie in ooreenstemming met die proses van deurlopende fraksionasie in die magmakamer nie. Die geleidelike toevoeging van ongedifferensieerde magma gedurende die kristallisatie van die boonste deel van Subson B, gevolg deur 'n groter, skielike indringing van magma op die vlak van die Piroksenietmerker, is heel waarskynlik verantwoordelik vir die waargenome verwantskappe.

CONTENTS

	PAGE
I INTRODUCTION .. .. .	1
II GENERAL GEOLOGY .. .. .	3
III LABORATORY TECHNIQUES .. .. .	9
1 Modal analyses .. .. .	9
2 Optical determination of the orthopyroxenes .. .. .	9
3 Optical determination of the plagioclase feldspars .. .. .	9
4 Chemical analyses .. .. .	10
4.1 Sample preparation .. .. .	10
4.2 Separation of the minerals .. .. .	11
4.3 Methods of analyses .. .. .	12
4.4 Calibration .. .. .	12
4.5 Accuracy .. .. .	13
5 Trace-element analyses .. .. .	16
5.1 Atomic absorption spectrometry .. .. .	16
5.1.1 Sample preparation and procedure .. .. .	17
5.2 Ion exchange chromatography spectrophotometry .. .. .	19
5.2.1 Sample preparation and procedure .. .. .	19
IV PETROGRAPHY .. .. .	22
1 Modal analyses .. .. .	22
2 Orthopyroxene .. .. .	26

	PAGE
2.1 Optical determination .. .. .	26
2.2 Chemical analyses .. .. .	28
2.3 Texture .. .. .	31
3 Plagioclase .. .. .	31
3.1 Optical determination .. .. .	31
3.2 Texture .. .. .	32
4 Whole-rock chemical analyses .. .. .	34
5 Discussion .. .. .	34
V TRACE-ELEMENT GEOCHEMISTRY .. .. .	41
1 Introduction .. .. .	41
2 Partitioning of the trace-elements .. .. .	42
2.1 Barium .. .. .	43
2.2 Chromium .. .. .	44
2.3 Cobalt .. .. .	48
2.4 Copper .. .. .	50
2.5 Nickel .. .. .	51
2.6 Strontium .. .. .	52
2.7 Vanadium and titanium .. .. .	54
2.8 Zinc .. .. .	58
3 Discussion .. .. .	60
VI SUMMARY AND CONCLUSIONS .. .. .	62
VII ACKNOWLEDGEMENTS .. .. .	65

PAGE

REFERENCES .. .. .	66
APPENDIX I .. .. .	72
APPENDIX II.. .. .	80
APPENDIX III .. .. .	82
APPENDIX IV.. .. .	84

TABLES AND FIGURES

	PAGE
Table I      Chemical composition of calibration standards for the analyses	14
Table II     Conditions during the analysis for the various elements by atomic absorption spectrometry	18
Fig. 1       The Bushveld Complex in the Eastern Transvaal, showing the four localities A,B,C and D, from where the samples for this investigation were obtained	2
Fig. 2       Localities of samples collected on Thornhill 544KS	4
Fig. 3       Localities of samples collected on Mapochsgronde 500JS (Roosenekal and Galgstroom )	5
Fig. 4       Localities of samples collected on Mapochsgronde 500JS ( Tonteldoos)	6
Fig. 5       Comparison of the optically and chemically determined composition of the orthopyroxenes	15

Fig. 6	Subdivision of gabbroic rocks	23
Fig. 7	Stratigraphical sections and modal analyses of rocks from the four localities	24
Fig. 8	Vertical variation in iron enrichment expressed as percentage ferrosilite in orthopyroxene	27
Fig. 9	The Ca - Mg - Fe quadrilaterals for the pyroxenes at the four localities	29
Fig. 10	Variation in composition of plagioclase (mol % An) and orthopyroxene (mol % Fs) from existing optical data	33
Fig. 11	Comparison of coexisting cumulus orthopyroxene (mol % Fs) and plagioclase (mol % An) from existing optical data	36
Fig. 12	Barium values for separated plagioclase and whole-rock	45

Fig. 13	Chromium values for orthopyroxene, clinopyroxene and whole-rock	47
Fig. 14	Cobalt values for orthopyroxene, clinopyroxene and whole-rock	49
Fig. 15	Nickel values for orthopyroxene, clinopyroxene and whole-rock	53
Fig. 16	Strontium values for plagioclase and whole-rock	55
Fig. 17	Titanium and vanadium values for whole-rock	57
Fig. 18	Zinc values for orthopyroxene, clinopyroxene and whole-rock	59

## I INTRODUCTION

Petrographical investigations by Von Gruenewaldt (1973b) and by Molyneux (1974) of the layered sequence above and below the Pyroxenite Marker, which forms the base of Subzone C of the

Main Zone of the Bushveld Complex have shown a compositional break in the cryptic layering at the level of the Pyroxenite Marker. Von Gruenewaldt (1973b, p.214) suggested that an influx of fresh, undifferentiated magma to the already partially differentiated residual magma was responsible for this compositional break.

The main object of the present research was, firstly, to investigate this compositional break in greater detail in order to establish whether an influx of magma could have been responsible for the break, and secondly, to determine any lateral variations that may be present at this level in the intrusion. For this purpose samples were collected along three traverses, two of which cross the Pyroxenite Marker and the third at the same stratigraphical height in an area where the Pyroxenite Marker is not developed. A borehole core containing the Pyroxenite Marker and the associated over- and underlying rocks from a fourth locality was also available.

The regional map (Fig.1) indicates the general location of the four areas from where the samples were obtained.

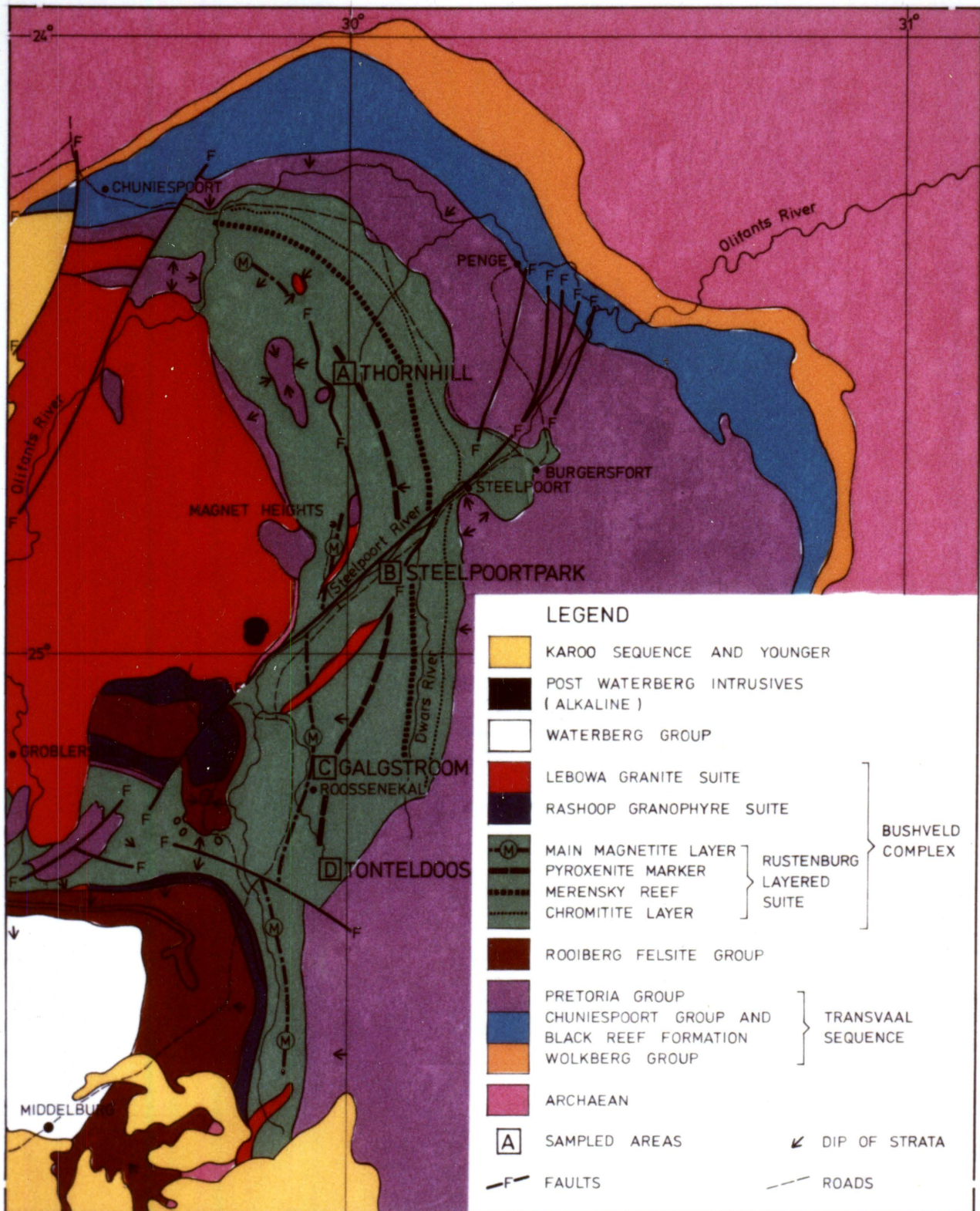


FIG.1 THE BUSHVELD COMPLEX IN THE EASTERN TRANSVAAL SHOWING THE FOUR LOCALITIES A,B,C & D FROM WHERE THE SAMPLES FOR THIS INVESTIGATION WERE OBTAINED

MAP BASED ON THE GEOLOGICAL MAP OF THE REPUBLIC OF SOUTH AFRICA [ 1970 ]

SCALE

KILOMETRES 0 10 20 30 40 50 60 70 80 90 100 110 120 130 140 150

They are :

- A. On the farm Thornhill 544KS, in Sekhukhuneland, where samples were collected at approximately 250 m intervals, along a road crossing the Pyroxenite Marker (Fig. 2).
- B. On the farm Steelpoortpark 366KT, 50 km north of Roossenekal, from a borehole drilled by the Phelps Dodge Corporation. This core was made available to the Department of Geology of the University of Pretoria. It is 584,6 m in length and intersects parts of Subzone B and Subzone C of the Main Zone. Between 210 m and 225,5 m depth, 12,5 m of this core was missing.
- C. Along the road from Roossenekal to Lydenburg, on the farm Mapochsgronde 500JS, as well as along the Galgstroom river, which runs parallel to the road 10 km further north, samples were collected at approximately 500 m intervals (Fig.3).
- D. Along the road to Tonteldoos, north-east of Stoffberg, on the farm Mapochsgronde 500JS, samples were collected at intervals of approximately 500 m (Fig. 4).

## II GENERAL GEOLOGY

Wager and Brown (1968) described the rocks of the Main Zone of the Bushveld Complex as being of gabbroic appearance, containing two pyroxenes and a plagioclase feldspar. They

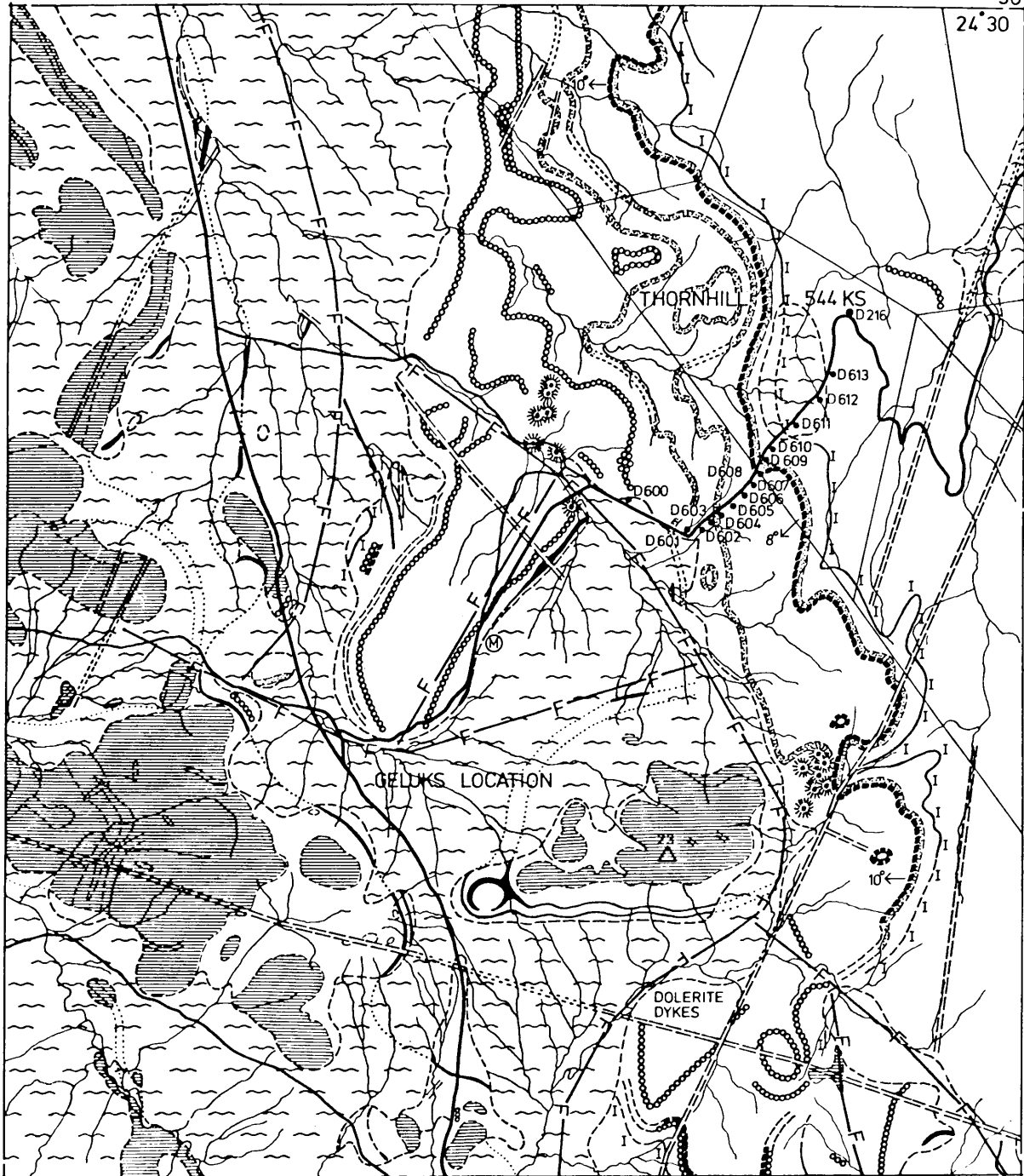
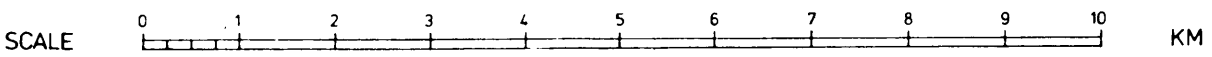
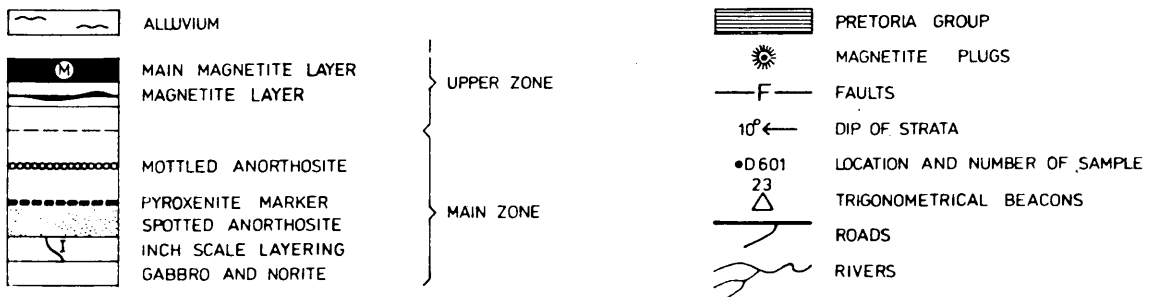


FIG. 2 LOCALITIES OF SAMPLES COLLECTED ON THORNHILL 544 KS AND ADJOINING GELUKS LOCATION SEKHUKHUNELAND GEOLOGY AFTER T.G. MOLYNEUX 1974



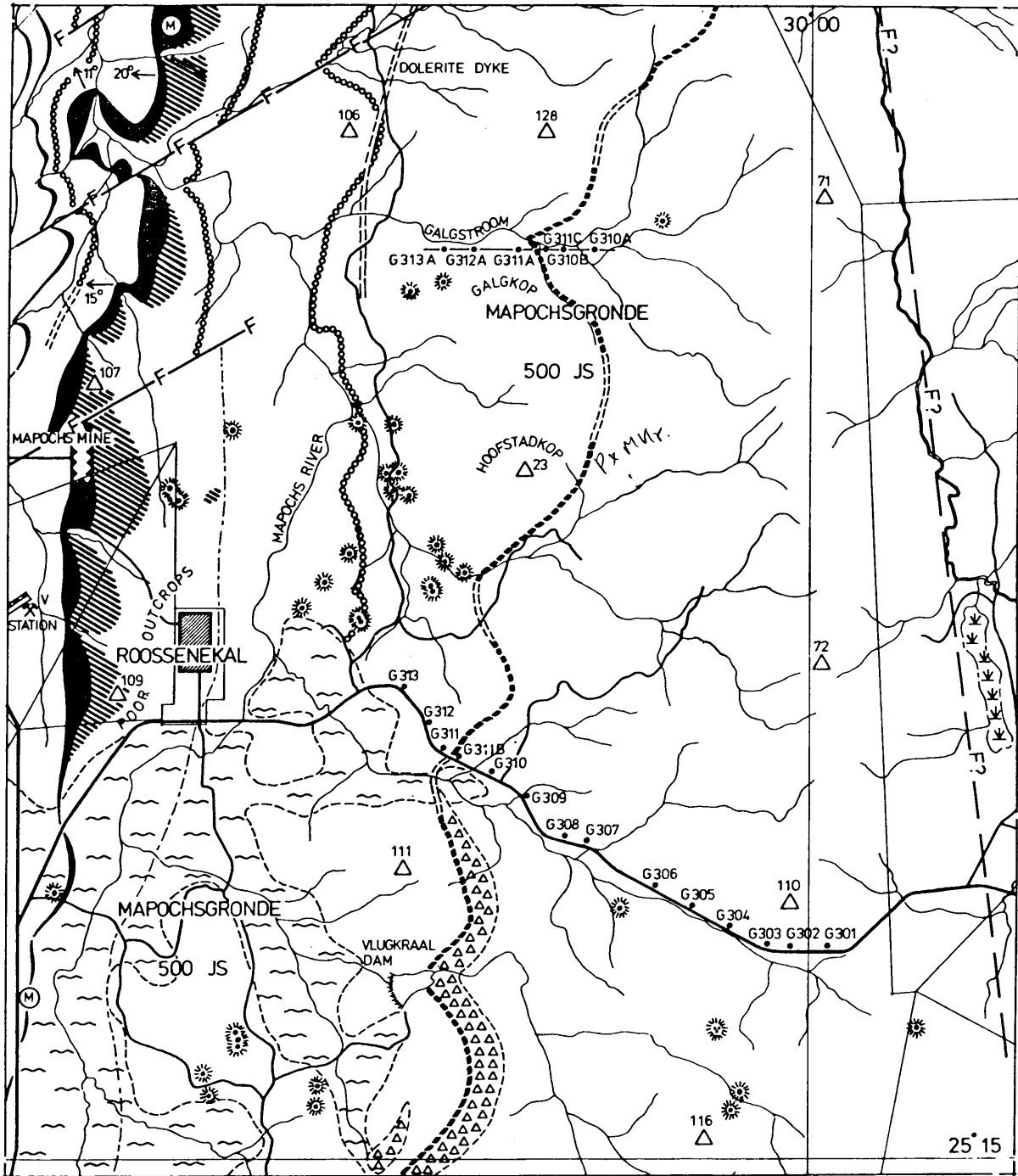
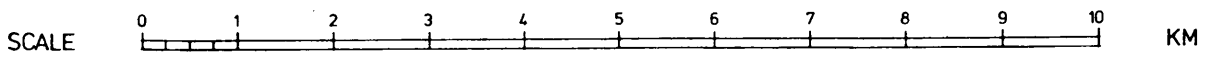
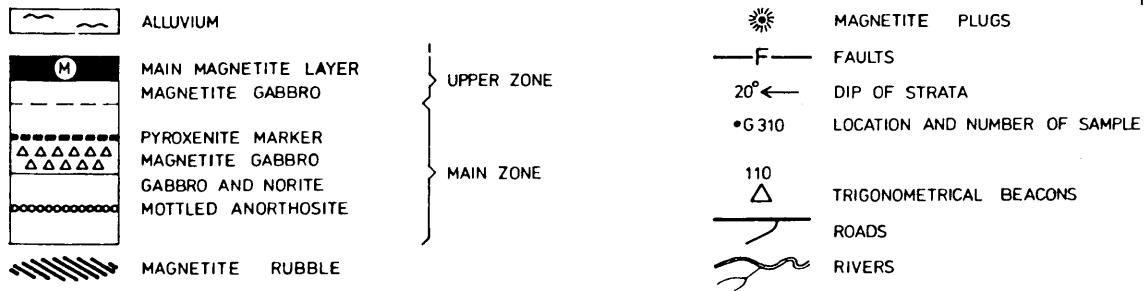


FIG. 3 LOCALITIES OF SAMPLES COLLECTED ON MAPOCHSGRONDE 500 JS  
VICINITY ROOSSENEKAL

GEOLOGY AFTER G. VON GRUENEWALDT  
1973 b



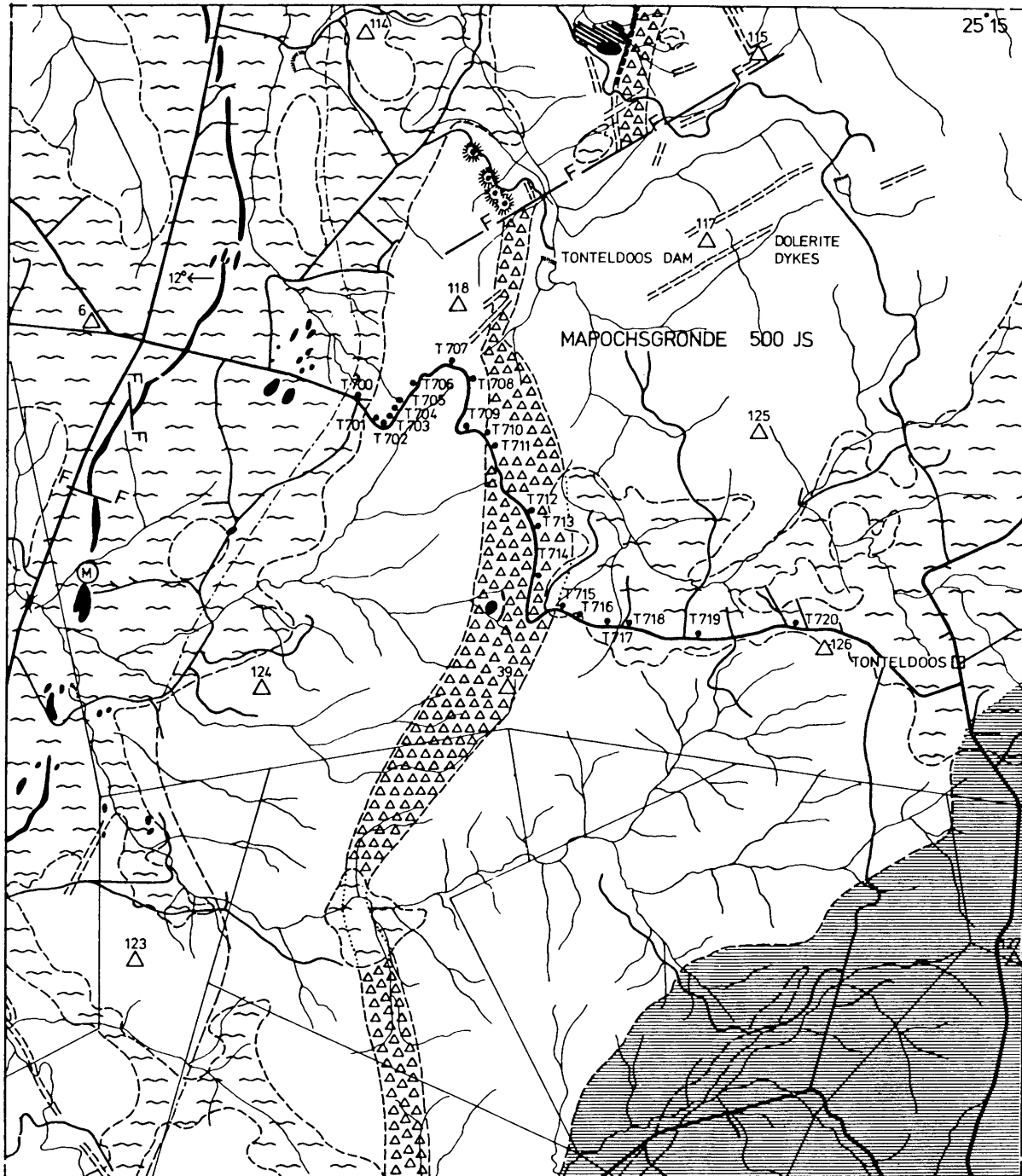
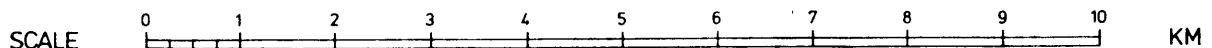
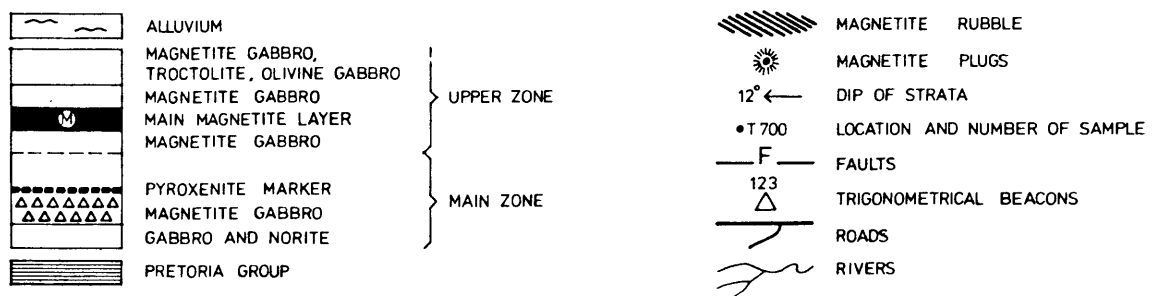


FIG. 4 LOCALITIES OF SAMPLES COLLECTED ON MAPOCHSGRONDE 500 JS  
VICINITY TONTeldoos GEOLOGY AFTER D. GROENEVELD 1970



estimated the total thickness to be approximately 2860 m, measured from the Merensky Reef at the base of the zone, to the first magnetite anorthosite just below the Main Magnetite layer. The Main Zone was subsequently subdivided by Von Gruenewaldt (1973b) and by Molyneux (1974) into three Subzones. The lower of these, Subzone A, consists of pyroxenite and gabbro-norite as well as mottled and spotted anorthosite. This Subzone is followed by Subzone B, which is a thick sequence of homogeneous gabbro-norite. The Pyroxenite Marker forms the base of Subzone C, which is some 690 m thick and which can be considered a repetition of the rock types encountered in Subzones A and B (Von Gruenewaldt, 1973b, p.208).

In the current project only the upper part of Subzone B and the lower part of Subzone C were examined, i.e the rocks directly above and below the Pyroxenite Marker of the Main Zone in the eastern Transvaal. The Pyroxenite Marker is a coarse-grained plagioclase-bearing pyroxenite, which can be followed for many kilometres along strike (Fig.1), and is found roughly three quarters of the way up in the Main Zone. This pyroxenite usually overlies a 100 m thick layer of fine-grained gabbro-norite which forms the top of Subzone B and which may contain some cumulus magnetite, but also some sulphides in the south. At Thornhill 544KS in Sekhukhuneland this fine-grained gabbro-norite is not developed, and only traces of magnetite

are present in the rocks directly below the Pyroxenite Marker. At Thornhill 544KS and Steelpoortpark 366KT, a second pyroxenite layer is developed above the Pyroxenite Marker. The Pyroxenite Marker was not found in the south at Tonteldoos, but Groeneveld (1970, Fig. 1) recorded a compositional break in the cumulus phases of the sequence directly above the fine-grained orthopyroxene gabbro. The clinopyroxene norite which is developed above the fine-grained orthopyroxene gabbro at Tonteldoos was taken to correspond to the Pyroxenite Marker farther north.

The gabbro-norite of Subzone B is easily identified in the field, owing to the reflection of sunlight on the cleavage planes of the grains of inverted pigeonite which are characteristically optically continuous over large areas.

The major features and the geology of the areas under discussion have been outlined by Groeneveld (1970), Von Gruenewaldt (1973b) and Molyneux (1974). Consequently the lithological description will not be dealt with in detail. Fig. 7 is a schematic illustration of the lithology at the four localities. The Pyroxenite Marker was taken as the datum, and distances (corrected for angle of dip) are shown as positive or negative values, corresponding to heights above and below this datum line respectively.

### III LABORATORY TECHNIQUES

#### 1 Modal analyses

Thin sections were analysed by means of a Swift Automatic Point Counter; the results are given in Appendix I. The number of points counted varied between 1300 and 1500 per thin section over an area of approximately  $340 \text{ mm}^2$ .

#### 2 Optical determination of the orthopyroxene

The composition of the orthopyroxene was determined by means of  $2V_x$ . The thin sections were cut normal to the igneous layering of the rock specimens in an attempt to obtain crystals with a suitable orientation for the measurement of  $2V_x$ . A universal stage with small glass hemispheres and a high-powered objective for conoscopic illumination were utilized. Only axial figures showing both isogyres were used, an average value was obtained from measurement on five grains in each thin section. After correcting the angle on Von Fedorow's nomogram (Tröger, 1959, p.123), the molecular percentage of ferrosilite was evaluated from the diagram of Tröger (1959, p.59).

#### 3 Optical determination of the plagioclase feldspars

The composition of the plagioclase feldspars was established optically by means of  $2V$  measurements on crystals

which allowed direct measurement of both optical axes. Conoscopic illumination was also employed in this case, and on average the 2V of five grains per thin section were determined. The molecular percentage of the anorthite in the plagioclase was obtained from the migration curves given by Burri, Parker and Wenk (1967).

Extinction angles were measured on at least ten Albite twins per thin section, using the method of Michel-Lévy (Kerr 1959, p.258).

#### 4 Chemical analyses

##### 4.1 Sample preparation

Samples of whole-rock, each weighing approximately 1 kg, were prepared as follows: All weathered surfaces were chipped off, and the borehole cores were scoured with rough sandpaper to remove any possible contamination from drilling operations. All samples were then broken down to approximately 0,5 cm diameter. The crushed samples were then divided roughly into two portions; one for whole-rock major and trace-element analyses, and the other for the separation of minerals on which major and trace elements were determined. The samples for chemical analyses were then ground to -340 mesh in a tungsten carbide mill.

A small portion of every sample was ground and discarded prior to grinding the bulk of the material, to ensure that contamination from previously ground samples did not take place. Samples were dried in an oven for 24 hours, and subsequently pelletised. Pellets were stored in a desiccator until analysed.

#### 4.2 Separation of the minerals

The samples used for mineral separation were pulverized by means of an agate mortar and pestle to pass a 100-mesh stainless steel sieve. The samples were wet-screened thoroughly at 200-mesh to remove all fine particles not amenable to dry magnetic separation.

The minerals were then separated by means of the Frantz Isodynamic Separator. The augite separated easily, because it is less magnetic than the coexisting hypersthene. The inverted pigeonite and the augite were first separated roughly to determine the most effective side slope for optimum concentration. The side slope and the current were then changed gradually, until the inverted pigeonite alone was being extracted on the magnetic side of the chute. Augite was concentrated on the less magnetic side by lowering the current to a point where the first augite just began to appear on the less magnetic side of the chute. This procedure was

repeated four times for each sample, until a reasonable concentrate was obtained. Microscopic examination of the grains after separation revealed that the plagioclase, which is diamagnetic, was virtually free from contamination by other minerals, whereas the orthopyroxene and the clinopyroxene had less than five per cent impurities.

#### 4.3 Methods of analyses

The analyses for major elements on the whole-rock and the separated pyroxenes were carried out by means of energy dispersive analysis of x-rays (EDAX) on the Philips XS-12-180 EXAM II of the Geological Survey. A high-power x-ray tube was used as source of primary radiation, in conjunction with a tungsten target. The analyzer, a Philips model 707A, is a multi-channel distribution analyzer which processes, channels and stores x-ray spectral data. A beryllium spectrometer was employed. The detection limit for the different major elements is about 1-50 ppm and the measurement time for quantitative analysis was 100 seconds.

#### 4.4 Calibration

Separate calibration curves had to be drawn for the pyroxene and the whole-rock analyses respectively. The standards chosen for the calibration curves had the same matrix as that of the samples analyzed, namely pyroxenite

(NIM P and NF4), norite (NIM N and NF8), andesite (AGV) and basalt (BCR) for the whole-rock analyses, and augite (Canada), diopside (U.S.A), hypersthene (Canada) and hornblende (Norway) for the pyroxene analyses (Table I).

The method of analysis and the calibration techniques, as well as the analytical procedure, are described fully in the manual which accompanies the Philips XS-12-180 EXAM spectrograph (Russ, 1972):

#### 4.5 Accuracy

The determination of the major elements of the pyroxenes using the EDAX-method should produce a high level of precision having a reproducibility with a variance of less than one per cent. The structural formulae of the pyroxenes were calculated according to the method given by Deer, Howie and Zussman (1969, p.515) and most analyses produced the precision normally required for a satisfactory analysis, i.e the number of cations to six oxygen atoms in the (WXY)-groups were within 0,02 of 2,00( APPENDIX II ). The values obtained by optical methods were plotted against those recalculated from the chemical analyses and a straight line was fitted by least squares regression, giving a correlation coefficient of 0,97966, thus implying close correspondence of determinative accuracy between the two methods (Fig. 5)

TABLE I                      CHEMICAL COMPOSITION OF CALIBRATION STANDARDS FOR THE ANALYSES

	BCR	NIM P	NIM N	AGV	NF 8	NF 4	N1/P1	AUG	DIOP	HYP	HORN
SiO <sub>2</sub>	54,50	51,18	52,65	59,00	50,47	54,52	51,93	51,70	54,44	51,06	51,44
TiO <sub>2</sub>	2,20	0,20	0,20	1,04	0,94	0,07	0,20	1,49	0,11	5,29	1,25
Al <sub>2</sub> O <sub>3</sub>	13,61	4,27	16,47	17,25	15,45	2,15	10,35	15,16	0,63	17,93	5,12
FeO	13,40	12,78	8,95	6,76	11,89	9,94	10,84	19,24	2,94	1,52	8,27
MnO	0,18	0,22	0,18	0,09	0,18	0,18	0,20	9,98	0,13	24,68	0,04
MgO	3,46	25,35	7,56	1,53	6,95	31,46	16,38	2,45	16,47	0,17	18,14
CaO	6,92	2,67	11,47	4,90	11,16	1,66	7,11	0,04	24,11	0,03	10,52
Na <sub>2</sub> O	3,27	0,38	2,47	4,26	2,39	0,19	1,41	0,11	0,74	0,36	2,40
K <sub>2</sub> O	1,70	0,09	0,25	2,89	0,85	0,08	0,17	0,41	0,02	0,26	0,38
Cr <sub>2</sub> O <sub>3</sub>	0,03	3,46	0,01	1,73	0,03	0,09	1,73	0,01	0,01	0,19	-
Total	99,27	100,60	100,21	99,45	100,29	100,34	100,32	100,59	99,60	101,49	97,56

BCR	Basalt	U.S. Geological Survey
NIM P	Pyroxenite	National Institute for Metallurgy
NIM N	Norite	National Institute for Metallurgy
AGV	Andesite	U.S. Geological Survey
NF 8	Norite	Geological Survey of S.A.
NF 4	Pyroxenite	Geological Survey of S.A.
N1/P1	Norite and pyroxenite	Geological Survey of S.A.
AUG	Augite	Referenco Co., Canada
DIOP	Diopside	Petcanine, New York, U.S.A.
HYP	Hypersthene	Labrador, Canada
HORN	Hornblende	Norway
	Reference standard	Boric acid

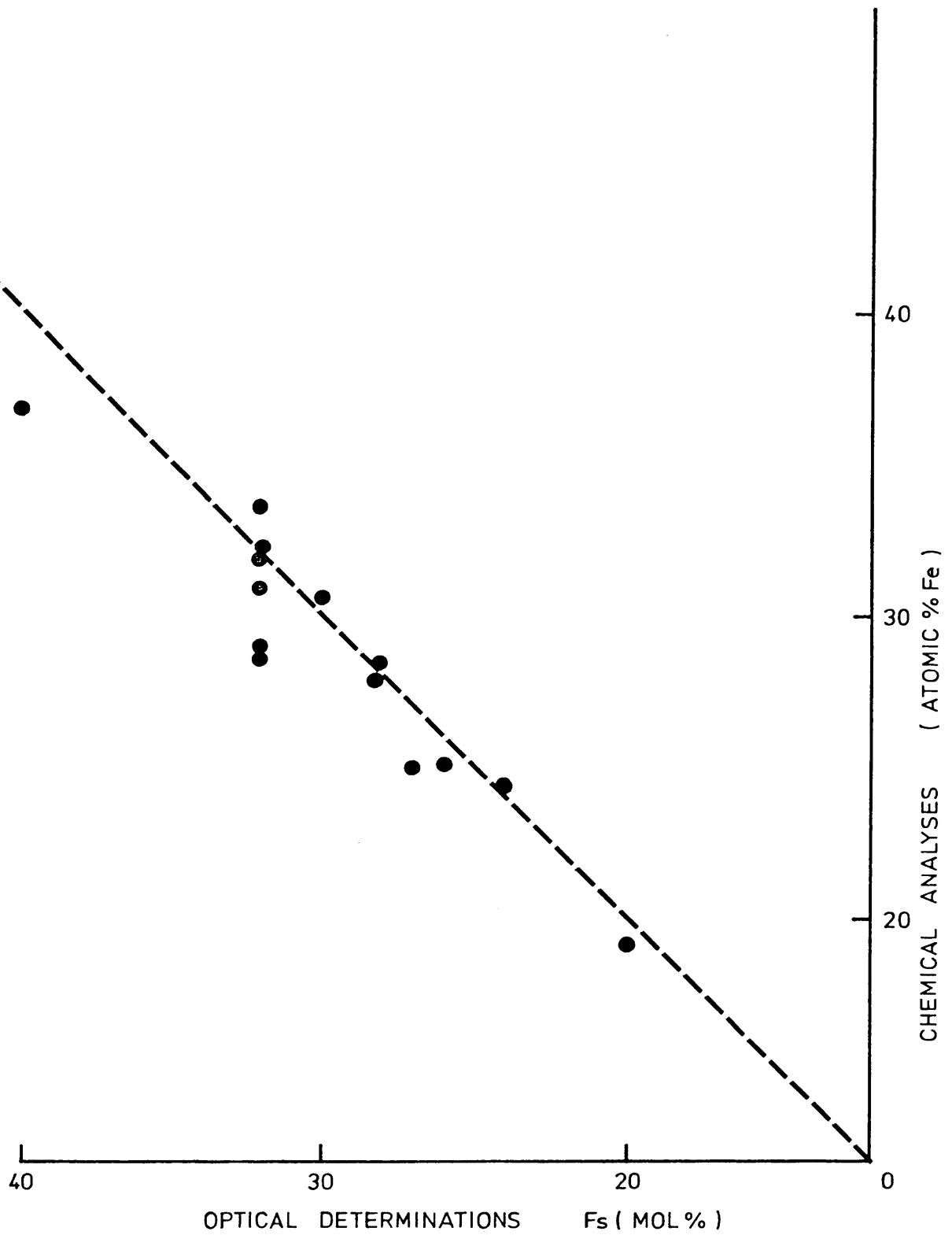


FIG.5 COMPARISON OF THE OPTICALLY AND CHEMICALLY DETERMINED COMPOSITION OF THE ORTHOPYROXENE

## 5 Trace-element analyses

The clean concentrates of the individual cumulus minerals and the coarsely crushed samples of whole-rock, were individually reground with an agate mortar and pestle to pass the 200-mesh sieve. This precaution was taken to avoid any possible contamination of the samples by trace elements which could be present in the metal of the tungsten carbide mill.

### 5.1 Atomic absorption spectrometry

The advantage of atomic absorption spectroscopy is the high sensitivity with which the presence of certain elements can be determined. The commercial equipment is comparatively simple to operate ( Kirkbright and Sargent, 1974, p.472 ) and a high precision and accuracy can be obtained with the aid of suitable calibration curves.

The sensitivity attainable for the determination of an element by AAS with a given instrument is defined as the concentration of the element (usually ppm) which produces a one per cent absorption signal ( 0,0044 absorbance) under optimum experimental conditions. The sensitivity value depends on the length of the absorption path, and on the efficiency of nebulization and atomization in the absorption cell. The degree of sensitivity is reflected by the

linearity of the calibration graph of absorption plotted against concentration (Robinson, 1966).

#### 5.1.1 Sample preparation and procedure

The method outlined by Belt (1964, p. 240) was followed to dissolve the samples. Several standard solutions of different concentrations were used ( i.e distilled water, 5 ppm, 10 ppm and 100 ppm ) to construct a calibration graph from which the signal strength could be related to concentration. Even when the calibration graph was not perfectly linear an increased number of standard solutions still permitted quite accurate analyses to be made. Standard solutions were nebulized each time after 10 samples had been examined to ensure that inaccurate analysis did not result from factors such as wavelength drift, change in the fuel to oxidant flow rate ratio, or variable nebulizer performance. The conditions during analysis for individual elements are given in Table II.

As a general test of the reproducibility of the trace-element determinations, the analyses were carried out on two different occasions. Small variations in the readings were registered for individual runs, but the deviations were never greater than five per cent. Because of this fluctuation, emphasis was placed on the relative magnitude of values obtained rather than on the values themselves.

TABLE II      CONDITIONS DURING THE ANALYSIS FOR THE VARIOUS  
ELEMENTS BY ATOMIC ABSORPTION SPECTROMETRY

Element	Wavelength	Flame	Slit	Remarks
Ba	553,56 nm	Nitrous oxide acetylene	1,0 mm	Interference by calcium. Precision for analysis $\pm$ 20 ppm.
Cr	357,87 nm	Nitrous oxide acetylene	0,1 mm	A narrow slit opening was used to give higher sensitivity.
Co	240,72 nm	Air-acetylene	0,1 mm	A decrease in slit width increases sensitivity, but at the expense of a noisier signal.
Cu	324,75 nm	Air-acetylene	0,3 mm	Copper is readily determined, sensitivity decreases at high current.
Ni	232,00 nm	Air-acetylene	0,1 mm	A narrow slit opening was used to minimize the transmission of nearby non-absorbing lines. A fuel-lean flame was used to give freedom from interferences especially in the presence of Fe and Cr.
Sr	460,73 nm	Nitrous oxide acetylene	0,2 mm	LaCl <sub>3</sub> was added to samples and standards to suppress ionization and residual chemical interference.
Zn	213,86 nm	Air-acetylene	2,0 mm	Fuel flow rate was closely regulated, and the sensitivity increased by using lower air-acetylene pressures than recommended.

The elements which were measured quantitatively by atomic absorption were barium, chromium, cobalt, copper, nickel, strontium and zinc.

## 5.2 Ion exchange chromatography-spectrophotometry

Owing to the serious interferences encountered, vanadium and titanium could not be determined successfully by atomic absorption spectrometry. These two elements were therefore determined on the whole-rock by means of ion exchange chromatography-spectrophotometry.

### 5.2.1 Sample preparation and procedure

The steps taken to prepare the solutions for analysis are described by Strelow (1963) and Strelow and Victor (1975) and comprised the following:

1 g of the sample was weighed into a teflon beaker. The sides of the beaker were washed with de-ionized water, and 10 ml concentrated perchloric acid and 10 ml concentrated hydrofluoric acid were added, (where the iron content of the samples was high, 1 ml 1 N hydrochloric acid was also added). The sample was fumed on a hotplate and the sides of the beaker were washed. This was repeated three times, after which it was evaporated to dryness at moderate heat ( ca. 200<sup>o</sup> - 250<sup>o</sup>C) and 20 ml concentrated perchloric acid ( ca. 10 N ) and two drops thirty per cent

hydrogen peroxide were added. The sample was then boiled until a clear solution was obtained, which was filtered into 400 ml flasks with de-ionized water. The insoluble residue left on the filter paper was fused with a mixture of NaOH and Na<sub>2</sub>O<sub>2</sub> and tested for Ti. No Ti could be detected. De-ionized water was added to the 400 ml graduation mark.

The cation exchange resin column was prepared as follows:

20 g dry cation exchange resin ( AG50W-X8 Bio-Rad ) was transferred to a column ( 20 cm diam) and brought into suspension with de-ionized water. The resin adhering to the inner walls of the column was washed down, and the de-ionized water was allowed to drain from the resin column. 100 ml 0,01 M nitric acid containing 0,15 per cent hydrogen peroxide solution (eluting agent A) was then added to the column and the solution was allowed to run through until approximately 10 ml was left above the resin column. The sample solution was then passed through the resin column quantitatively ; the flask and the column walls were rinsed down with the eluting agent A, and eluted into a clean 600 ml beaker. Al, Fe(III), Ti(IV), Ca, Mg, Mn(II) and Na etc are retained on the

column, whereas the vanadium (as V(V)) is quantitatively eluted. The titanium (together with the alkali metals) was eluted into a clean beaker with 350 ml 1 N sulphuric acid containing 1 per cent hydrogen peroxide, while the alkaline earth metals, Fe(III), Al(III) etc, remained on the column. For re-use, the columns were stripped of the remaining eluate with 500 ml HCl. The vanadium and titanium solutions were evaporated to dryness in a water bath and the following steps implemented to determine their respective concentrations:

The titanium (vanadium) residue was dissolved in 20 ml ( 2 ml ) 1:1 v/v H<sub>2</sub>SO<sub>4</sub> ( ca. 35 N ) and 10 ml ( 1 ml ) 3 per cent v/v H<sub>2</sub>O<sub>2</sub>, and the clear solution diluted to 100 ml ( 10 ml ) . The absorbance was measured at 410 ( 460 ) nm against water. The calibration curve was constructed from solutions containing 25, 50, 75 and 100 ppm Ti(IV) and V(V). In the case of V(V), the solutions were added to 3 ml H<sub>2</sub>O (de-ionized water) after the addition of H<sub>2</sub>SO<sub>4</sub> ( 1 ml 1:1 v/v ), and the absorbance was read at 460 nm to serve as a correction for possible Cr(III) which might accompany the V(V). It was assumed that the samples contained no Mo(VI) which can cause interferences.

#### IV PETROGRAPHY

##### 1 Modal analyses

Modal analyses were done in order to determine whether any vertical or lateral variations in the proportions of the constituents of the rock sequence could be detected. They were also used in selecting representative specimens for the trace-element and major-element analyses. Furthermore, the mode was also used as a basis for the quantitative classification of the rocks according to the scheme proposed by Streckeisen (1976) (Fig. 6).

The modal compositions of the rocks from the four localities (Appendix I and Fig. 7) revealed the following: The rocks from the traverse at Thornhill 544KS are mainly clinopyroxene norite and orthopyroxene gabbro and plagioclase-bearing pyroxenite. A second plagioclase-bearing pyroxenite is developed above the Pyroxenite Marker. The fine-grained magnetite-bearing rocks which usually underlie the Pyroxenite Marker in the south are not developed here, although magnetite is present in traces in a clinopyroxene norite which lies directly below the Pyroxenite Marker. The content of the plagioclase in the gabbroic rocks remains fairly constant at about 65 per cent. Of interest is the fact, that orthopyroxene predominates over clinopyroxene in the rocks of Subzone C in contrast with the rocks of Subzone B (Fig. 7A).

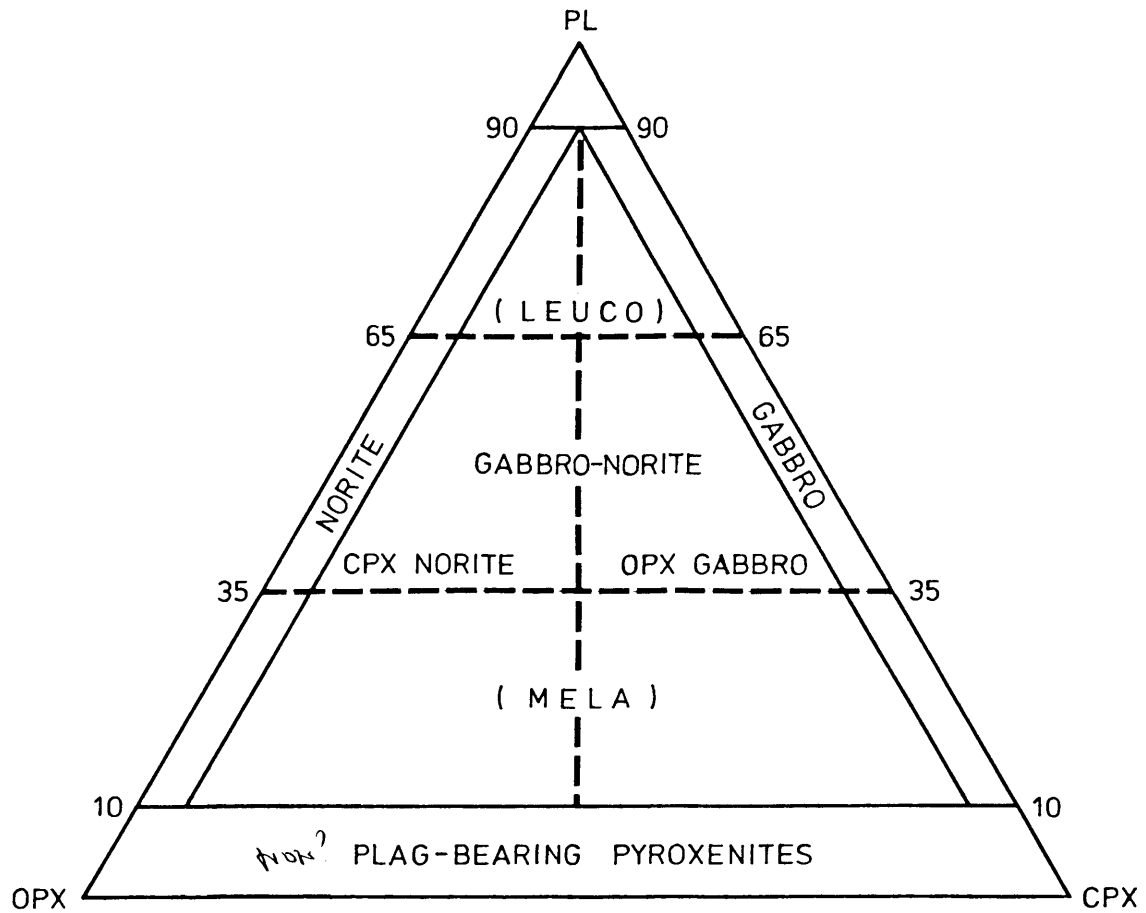


FIG.6 SUBDIVISION OF GABBROIC ROCKS  
AFTER STRECKEISEN, 1976

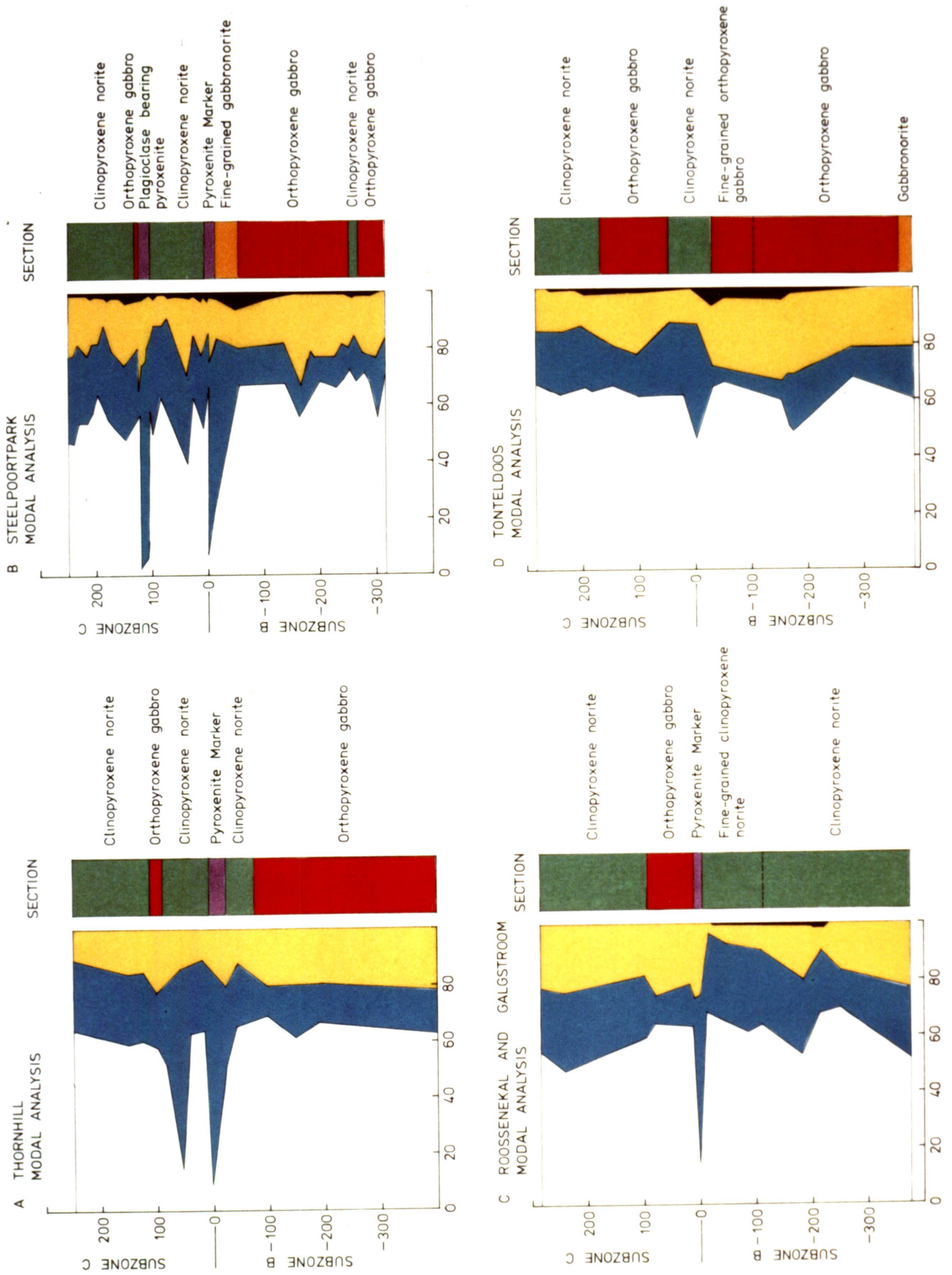


FIG. 7 STRATIGRAPHIC SECTIONS AND MODAL ANALYSES AT THE FOUR LOCALITIES

PLAGIOCLASE    
  ORTHOPYROXENE    
  CLINOPYROXENE    
  OPAQUE MINERALS

At Steelpoortpark 366KT (Fig. 7B) the Pyroxenite Marker lies directly above the fine-grained gabbro-norite is approximately 100 m thick and which may contain up to 5,6 per cent cumulus magnetite. Similar to the Thornhill 544KS traverse, clinopyroxene is the dominant ferromagnesian mineral in rocks of Subzone B, whereas it is orthopyroxene in the rocks above the Pyroxenite Marker. Also, there is a noticeable drop in the plagioclase content of approximately 65 per cent in Subzone B to about 55 per cent in Subzone C.

At Roossenekal (Fig. 7C) a fine-grained clinopyroxene norite, some 100 m thick is developed below the Pyroxenite Marker and contains cumulus magnetite. A second plagioclase-bearing pyroxenite is not developed in this area although Von Gruenewaldt (1973b, p.209) found a second pyroxenite layer below the Pyroxenite Marker near the northern boundary of Mapochsgronde 500JS. In contrast with the two previous traverses, orthopyroxene predominates below the Pyroxenite Marker, whereas clinopyroxene shows a pronounced increase above this layer.

At Tonteldoos in the south (Fig. 7D) the fine-grained orthopyroxene gabbro contains up to 6,5 per cent magnetite as well as some sulphides. In this area Groeneveld (1970, p.39) noted that the plagioclase laths have a grey colour due to inclusions of numerous tiny rods of magnetite. Although

the plagioclase content remains fairly constant throughout, there is, as is the case in the Thornhill 544KS and Steelpoortpark 366KT sections, also a pronounced decrease in the clinopyroxene content from Subzone B to Subzone C.

Groeneveld (1970,p.39) recorded the predominance of orthopyroxene over clinopyroxene in the magnetite-bearing rocks.

## 2 Orthopyroxene

### 2.1 Optical determination

The composition of the orthopyroxene shows a reversal in the trend of iron enrichment with fractionation for all the areas, with a compositional break at the height of the Pyroxenite Marker, as well as in the correlated clinopyroxene norite layer in the south (Fig. 8). From Figures 8 and 10 it can be seen that the fractionation trend seems to be normal up to a level some 250 - 300 m below the Pyroxenite Marker. From here upwards the trend is reversed and continuous to the top of the sequence investigated in all four areas. From the work of Von Gruenewaldt (1973b, p.221) and Molyneux (1974, p.337) in the Roossenekal and Thornhill areas the reversal continues to about 350 m, and 750 m respectively above the Pyroxenite Marker before returning to normal. It is also evident that the ferrosilite content of the orthopyroxene of the Pyroxenite Marker, as well as of the over- and underlying rocks, increases towards the south (Fig.8).

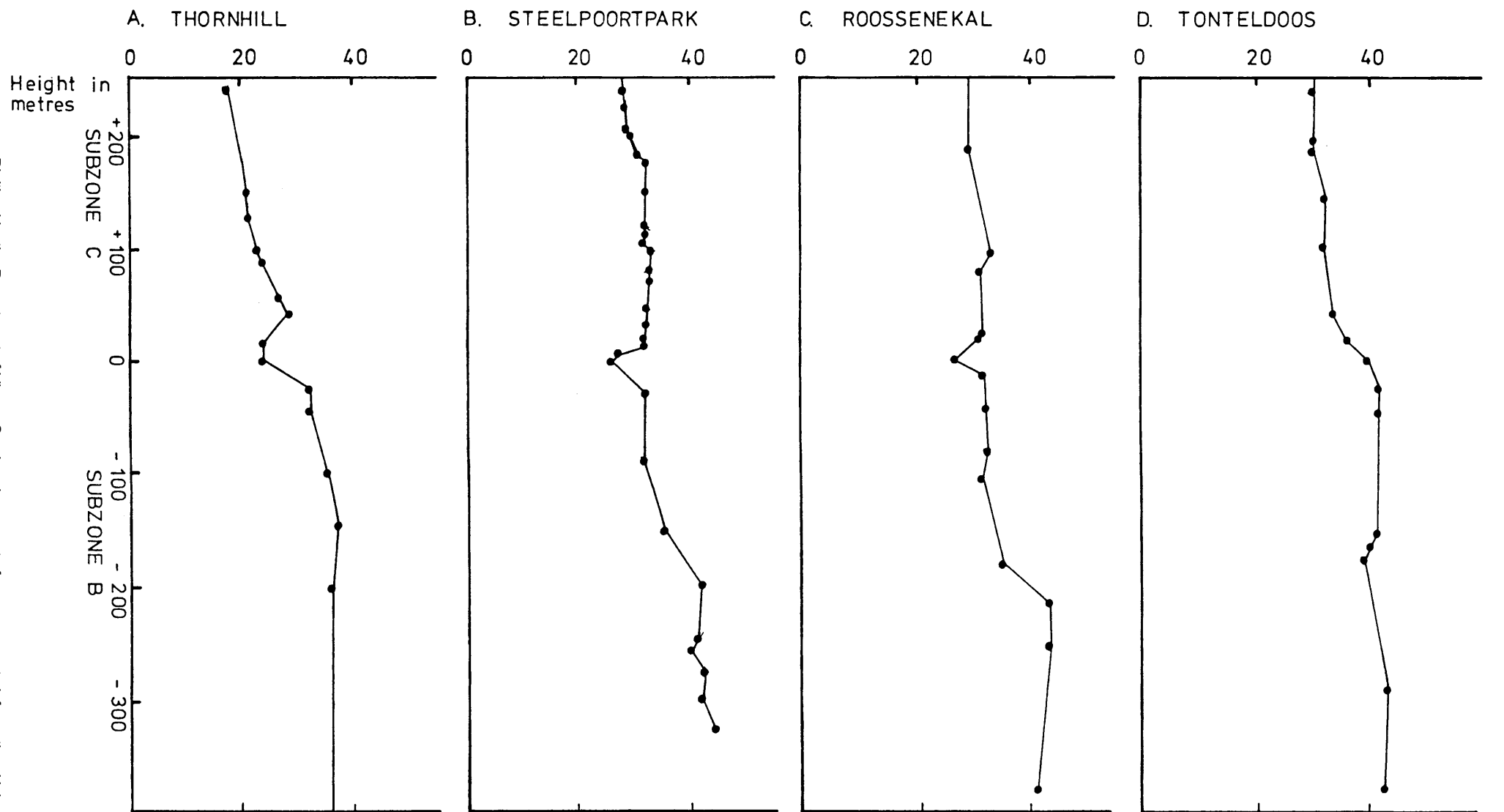


FIG. 8 VERTICAL VARIATION IN IRON ENRICHMENT EXPRESSED AS PERCENTAGE FERROSILITE IN ORTHOPYROXENE  
● OPTICAL DETERMINATION

## 2.2 Chemical analyses

Since the early work by Hess (1941) it has been accepted that the chemical composition of the pyroxenes, expressed in terms of  $\text{CaSiO}_3$ ,  $\text{MgSiO}_3$  and  $\text{FeSiO}_3$  can reveal important information on the fractionation trend of a tholeiitic magma.

The compositional variations of the pyroxene from the four localities in the eastern Transvaal are shown in Fig.9. Also plotted on this diagram are data for clinopyroxene from the eastern part of the Bushveld (Atkins, 1969), the western part of the Bushveld (Markgraaff, 1976) and data from borehole KLG/2 in the Bethal area (Buchanan, 1976).

The Ca-Mg-Fe ratios have been calculated from the pyroxene analyses in Appendix II. The tie-lines in Figure 9 indicate the coexisting pyroxene pairs. The calcium-rich pyroxenes show, in accordance with the results obtained by other investigators, a decrease in the Ca component with fractionation. They differ, however, in composition from those investigated by Atkins (1969) in that they are less calcic and therefore correspond more closely to those investigated by Buchanan (1976).

For pyroxene pairs of similar composition ( No.2, Fig.9A No.1, Fig.9B, No.1 Fig.9C and No.1 Fig. 9D) the immiscibility gap increases from Thornhill 544KS to Tonteldoos which can be explained by a lateral temperature gradient. This would have the effect that the pyroxene solidus would have been depressed in

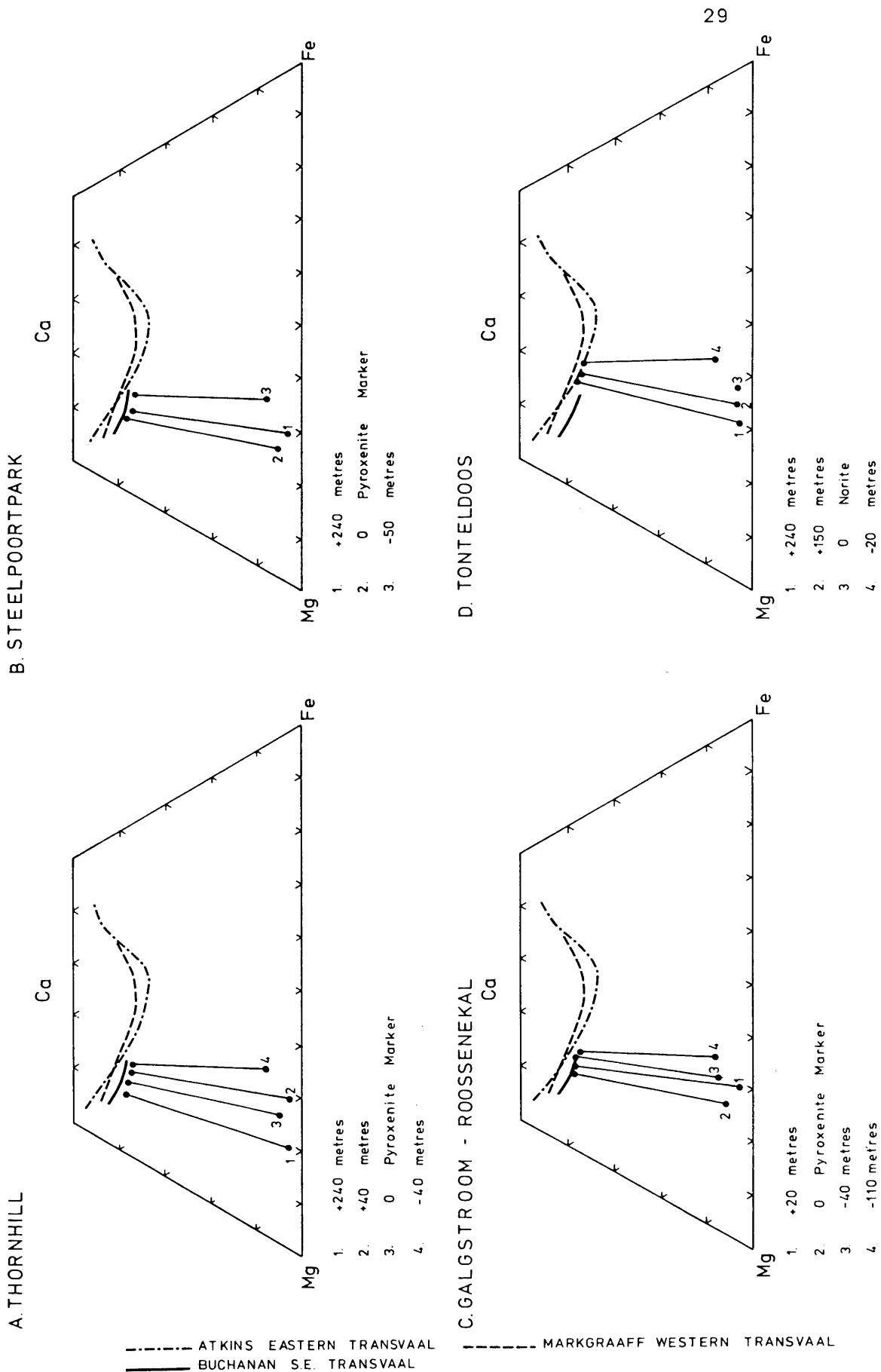


FIG. 9 THE Ca - Mg - Fe QUADRILATERALS FOR THE PYROXENES AT THE FOUR LOCALITIES.

the south relative to the north so that the solidus intersected the solvus at lower levels (i.e. apparently at lower temperatures). Because of the shape of the solidus (Barth, 1962, Fig. III-24) the immiscibility gap between coexisting pyroxene pairs at Tonteldoos would be slightly greater than for pyroxene pairs of similar compositions at Thornhill 544KS.

The primary orthopyroxene characteristically contains about 3 mol per cent Ca in contrast with the inverted pigeonite below the Pyroxenite Marker which contains approximately 8 mol per cent Ca. The primary orthopyroxene in all the samples from the Pyroxenite Marker contains more Ca than the primary orthopyroxene in the overlying gabbroic rocks. Although no reasonable explanation can be offered for this discrepancy at this stage, a higher Ca-content for the orthopyroxenes of the Pyroxenite Marker can result if it is assumed that the pyroxene of this layer crystallized at a higher temperature than the over- and underlying gabbroic rocks, thereby taking more Ca into solid solution. Conversely, Davis and Boyd (1966, p. 3567) found that the extent of the solid solution in the system  $\text{MgSiO}_3 - \text{CaMgSi}_2\text{O}_6$  greatly increased with increasing pressure. On the assumption that these findings can be extrapolated into the pyroxene quadrilateral it could be argued that the Pyroxenite Marker crystallized under conditions of higher pressure than the

over- and underlying gabbroic rocks. Such an increase in pressure could be envisaged during a forceful emplacement of a considerable quantity of fresh, undifferentiated magma into the chamber.

### 2.3 Texture

In all the areas the Ca-poor pyroxene below the Pyroxenite Marker is an inverted pigeonite. The inverted pigeonite is characterized by groups of grains having the same orientation, but the pre-inversion exsolution lamellae of augite have different orientations from grain to grain. Post-inversion exsolution lamellae are orientated parallel to the (100) direction of the inverted pigeonite, viz. the same orientation in all the grains of a particular cluster. This texture, and the possible origin thereof is described in more detail by Von Gruenewaldt (1970) and by Von Gruenewaldt and Weber-Diefenbach (1977).

Above the compositional break at the base of the Pyroxenite Marker the Ca-poor pyroxene is primary hypersthene, characterized by the exsolution striae of augite parallel to (100) of the orthopyroxene.

## 3 Plagioclase

### 3.1 Optical determination

The composition of the plagioclase is usually above

An<sub>65</sub> in the lower parts of Subzone B (Von Gruenewaldt, 1973b, Fig.16, Molyneux, 1974, Fig.8 and Groeneveld 1970, Fig.1,2 and 3)(Fig.10), gradually decreases to values below An<sub>60</sub> some 200 - 300 m below the Pyroxenite Marker, and then increases to values of An<sub>70</sub> or more above the Pyroxenite Marker. At the level of the Pyroxenite Marker the composition increases rapidly by about 5 mol per cent anorthite, after which it increases more gradually. According to Von Gruenewaldt (1973b, p.221) this increase in the An-content continues for about 350 m above the Pyroxenite Marker before the normal fractionation trend is resumed right to the top of the intrusion.

The compositional trends recorded in the orthopyroxene are thus also reflected by the ~~plagioclase~~ plagioclase. However, the lateral variations in the composition is not as pronounced as that of the orthopyroxene. The composition of the plagioclase and the orthopyroxene obtained in the current investigation as well as the values of Groeneveld (1970, Fig.1, 2 and 3 ), Molyneux (1974, Fig.8) and Von Gruenewaldt (1973b, Fig. 16) are indicated in Fig.10. This facilitates comparison of the results obtained and also provides additional information on the change in composition of the minerals below those sampled for this investigation.

### 3.2 Texture

The cumulus plagioclase feldspar exhibits textural

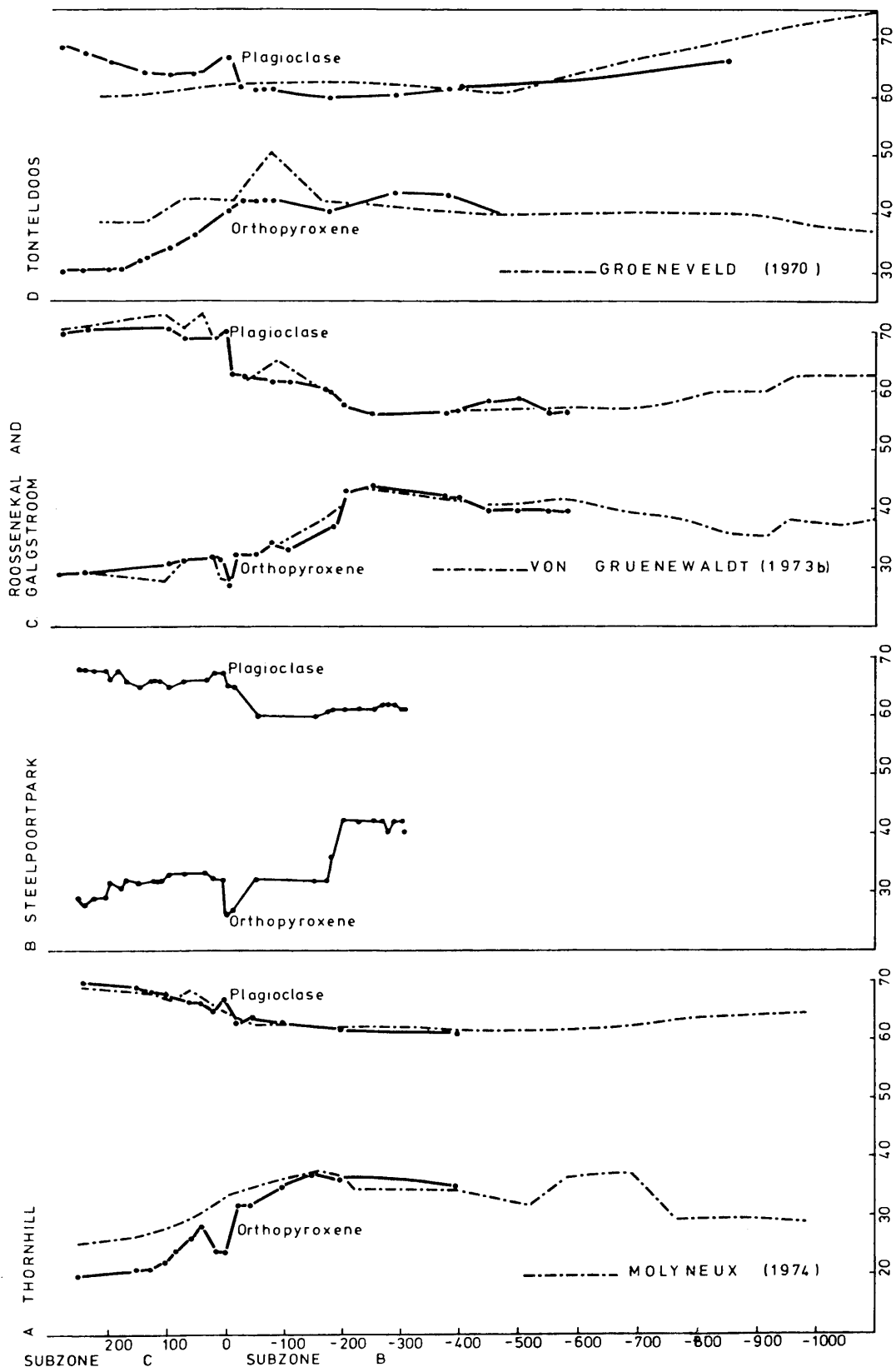


FIG.10 VARIATION IN COMPOSITION OF  
PLAGIOCLASE (MOL%AN) AND ORTHOPYROXENE (MOL%FS)  
FROM EXISTING OPTICAL DATA

features indicative of deformation after deposition. Bent crystals, interpenetration of adjoining cumulus crystals and myrmekitic intergrowths are present. Large quantities of myrmekite are present in the upper half of Subzone B, but absent where primary orthopyroxene is present in Subzone C. These textural features were investigated in greater detail by Von Gruenewaldt (1971, p.94). Furthermore, the plagioclase is zoned in practically all thin sections investigated. The zoning may be reversed, normal or oscillatory and is mostly confined to the outermost, narrow rims of the crystals.

#### 4 Whole-rock chemical analyses

The results of the whole-rock analyses, the modified differentiation index, modified crystallization index and the C.I.P.W.-norm, are tabulated in Appendix III. Although plots of the MDI and MCI against height in the intrusion were attempted these did not reveal any meaningful patterns. The reason for this is that the bulk compositions of the rocks in this part of the succession do not differ sufficiently to display any meaningful trends.

#### 5 Discussion

To compare the presently established fractionation

trends in the rocks with those found by Molyneux (1974), Von Gruenewaldt (1973b) and Buchanan (1975), the composition of the coexisting cumulus orthopyroxene and plagioclase, inferred from optical data, are shown in Fig.11 which is based on a diagram by Buchanan (1975, p.346).

For a certain anorthite content of the plagioclase, the iron content of the orthopyroxene decreases from south to north in the order Tonteldoos, Roossenekal and Galgstrom, Steelpoortpark 366KT and Thornhill 544KS. In the south the iron content of the orthopyroxene is even higher than that established by Von Gruenewaldt (1973b) and in the north the corresponding values are lower than those of Molyneux. Buchanan's explanation (1975, p.346) that the difference in the observed trends in Fig.11 between the Bethal area and the eastern Bushveld is a result of difference in oxygen fugacity, cannot be applied to the observed trends in the four sections investigated. Again, a lateral temperature gradient seems a more feasible explanation to account for the iron enrichment of the orthopyroxene in a southerly direction and that the pyroxene seems to be more sensitive to changes in temperature than the coexisting plagioclase.

A lateral cryptic variation in the composition of the orthopyroxene from the centre to the margin of the Great Dyke was observed by Hughes (1970, p.324). He considered this

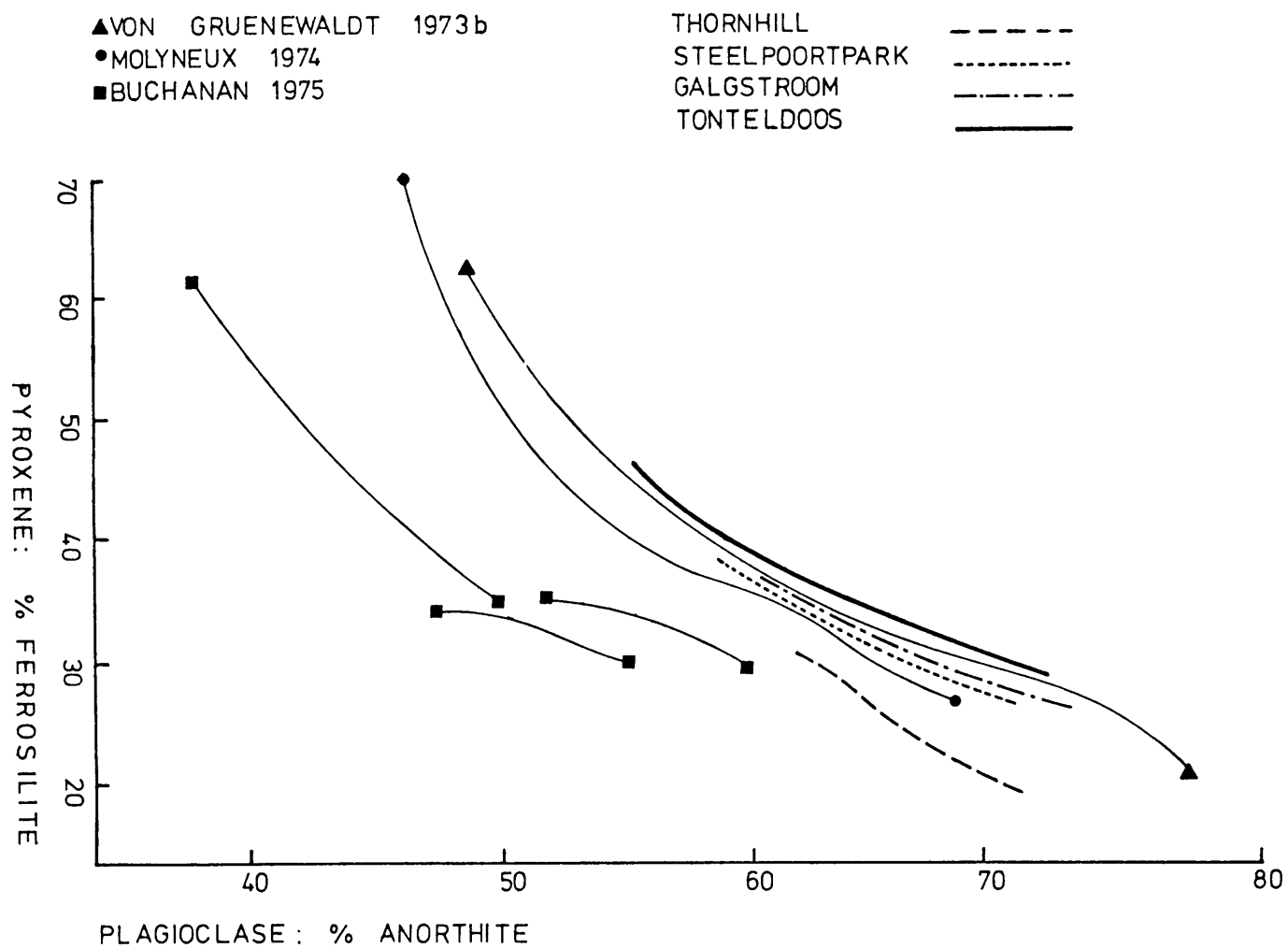


FIG. 11 COMPARISON OF COEXISTING CUMULUS ORTHOPYROXENE (mol % Fs) AND PLAGIOCLASE (mol % An) FROM EXISTING OPTICAL DATA

variation to be due to a more rapid decrease in temperature in the thinner, marginal area of the body of basic magma. Another possible explanation for the observed variation was suggested by Von Gruenewaldt (1973b, p.214) namely that an influx of fresh, undifferentiated magma in the central portion of the chamber could have pushed the existing differentiated magma outwards to the marginal areas. This would result in a change in composition of the magma from north to south.

The reversal in the crystallization pattern, as well as the compositional break indicates a disturbance of the normal trend of fractional crystallization of the Bushveld magma. Buchanan (1976, p.135) recorded a reversal in the fractionation trend at the base of the Upper Zone in the Bethal area. He proposed that the reason for this was that the magma was injected as a separate intrusion in this area. Atkins (1969, p.241) also mentions that small-scale reversals were detected by him and other research workers, the most important being at the base of the Merensky Reef.

Himmelberg and Ford (1976, p.232) recorded a marked reversal in the Fe/(Fe+Mg)-ratio in the pyroxenes of the Saratoga gabbro of the Dufek Intrusion in Antarctica. They were reluctant to interpret this anomaly because the reversal took place between samples taken from different sections that were separated by almost 6,5 km horizontally

and 100 m vertically.

There are many factors which could cause reversals in the differentiation trends within a sequence of layered igneous rocks. Intermittent heaves of undifferentiated magma have been suggested as one factor by Wager and Brown (1968, p.405). Cameron (1971, p.105) proposed that a gradual influx of undifferentiated magma and the subsequent mixing with the partially differentiated magma in the chamber would cause the progressive decrease of the Fs-content of the orthopyroxene upwards in parts of the Critical Zone as observed by him. From a similar, but more extreme, reversal in composition of coexisting cumulus minerals in the Main Zone Von Gruenewaldt (1973a, p.225) calculated that at least 10 per cent of the total volume of the Bushveld magma was added to the magma chamber immediately prior to crystallization of the Pyroxenite Marker of the Main Zone.

MacDonald (1967, p.185), in his study of the evolution of the lower portion of the Critical Zone on the farm Ruighoek, in the western part of the Bushveld Complex, found that the anorthite content in the plagioclase increased slightly but progressively with height, while the orthopyroxene revealed a reversal in the iron content. He was of the opinion that the composition could have been influenced by a separate intrusion of undifferentiated parent-magma, or by the settling of crystals formed near the top of the magma chamber. Because crystals

forming near the roof of the chamber would be richer in magnesium than the magma, the resorption of these crystals as they settled into regions of higher temperature would enrich the central zone of the magma in magnesium. The enriched zone would then enlarge as resorption of the crystals continued. The magnesium content of the crystals that formed near the floor would increase continually, as the zone enriched in magnesium gradually encroached on the zone of crystallization. The rate at which the central zones of the magma became enriched in magnesium would depend on conditions governing crystallization near the roof, and would not be affected by the rate of crystallization in the lower part of the magma chamber.

In the Stillwater Complex, Jackson (1970, p.401) established that the chemical variation found in the cumulus olivine in several cyclic units showed a steady decrease in iron content with height, which was followed by normal enrichment in iron. He cites similar features from the lower parts of other layered intrusions, notably the Bushveld Complex and the Great Dyke and comes to the conclusion that the unexpected iron depletion was due to the failure of the magma to reach complete equilibrium. This may be a feasible explanation for the reversal close to the base of layered complexes, but the reversal studied in this investigation

occurs at a very much higher level, where the magma should have been under equilibrium conditions for a considerable time.

The gradual onset of the reversal some 300 m below the Pyroxenite Marker would indicate that the influx of some magma took place well before crystallization of the Pyroxenite Marker and that this influx was gradual and that the subsequent mixing with the partially differentiated magma caused the reversal similar to that described by Cameron (1971, p.105). The more pronounced break at the Pyroxenite Marker could possibly be due to a sudden, more forceful injection of a larger quantity of magma, possibly accompanied by an increase in pressure as indicated by the increased Ca-component in the orthopyroxene. The continued reversal above the Pyroxenite Marker furthermore indicates that gradual additions of magma continued for some time after the formation of the Pyroxenite Marker.

From the distribution pattern of certain trace-elements, Irvine and Smith (1967, p.47) postulated that several influxes of fresh, undifferentiated magma occurred during crystallization of the Muskox intrusion. In view of their findings, that distribution patterns of trace-elements could be used as indicators of periodic additions of magma, such an investigation was attempted for the succession under consideration and is discussed in the next chapter.

V TRACE - ELEMENT GEOCHEMISTRY

1 INTRODUCTION

One of the most thoroughly documented accounts of trace-element fractionation during magmatic crystallization is that of the Skaergaard intrusion (Wager and Mitchell, 1951). Wager and Brown (1968, p.184) found that trace-elements often show a relatively greater change with fractionation than do major elements. Because of this, data on trace-elements could provide a better indication of the stage of fractionation represented by a particular rock than data on the major elements.

The trace-elements fall into three groups:

- i Elements which readily enter the early minerals; the concentration decreases with fractionation (eg. chromium and nickel).
  
- ii Elements which enter the cumulus minerals formed during the middle and late stages of fractionation; the concentration in the rocks rise to a maximum and then decrease (eg. cobalt and strontium).
  
- iii Elements which tend to remain in the residual liquid are most abundant in the rocks formed last (eg. barium) (Wager and Brown, 1968, p.183).

Trace-element analyses on separated cumulus minerals, as well as on whole-rock samples were done by atomic absorption spectrometry, with the exception of the elements vanadium and titanium, which were determined by ion exchange chromatography (Appendix IV).

## 2 Partitioning of the trace-elements

As the partition coefficient of trace-elements between the solid and the liquid is a function of temperature, pressure and composition of the crystallizing phase, it would be anticipated that enrichment or depletion in trace-elements in a residual magma would vary. The fractionation trends observed for certain ions between the magma and silicate minerals have been interpreted in terms of the crystal field theory by Burns(1970).

According to Burns (1970, p.9) the chemistry of the transition-metals is dominated by incompletely filled d-shells of the electron structure. The five 3d-orbitals ( $d_{xy}$ ,  $d_{yz}$ ,  $d_{xz}$ ,  $d_{x^2 - y^2}$  and  $d_{z^2}$ ) are degenerate when the transition-metal ion is isolated from ligands such as sulphur and oxygen. In the presence of these ligands, however, energy differences are created and splitting of the  $d_{xy}$ ,  $d_{yz}$  and  $d_{xz}$  -orbitals with respect to the  $d_{x^2 - y^2}$  -orbitals take place. The manner in which the splitting takes place depends on whether the ions are in octahedral or tetrahedral co-ordination in a quasi-crystalline

lattice. The induced separation of the 3d-orbitals is greater for octahedral symmetry than for tetrahedral symmetry, and the resultant stabilizing energy is called the crystal field stabilizing energy (CFSE). The difference between the octahedral and the tetrahedral CFSE for a given cation is termed the octahedral site preference energy (OSPE). The OSPE is useful in predicting the distribution of the transition-metals in structures containing both octahedral and tetrahedral sites, as it is energetically more favourable for them to be removed from tetrahedral co-ordination in a magma and to enter octahedral sites in minerals such as pyroxene and olivine.

The order of OSPE in oxides for divalent transition-metal ions is:

$Ni > Cu > Co > Fe > Mn \geq Ca, Zn$

and for the trivalent ions:

$Cr > Mn > Ti > Fe \geq Sc$

## 2.1 Barium

The geochemical behaviour of this element is comparatively simple since it substitutes only for  $K^+$  among common cations.  $Ba^{2+}$  is nearly identical in size with  $K^+$  (Ahrens et al., 1965, p.155). Ideally the barium content should rise in the residual liquid of a fractionating magma, and according to Wager and Brown (1968, p.194) the values

should be highest in the last differentiates; i.e. the intermediate and acid rocks of the intrusion.

In Subzone B (Fig.12) of the areas examined, the barium values of the rocks show an initial slight increase, followed by a decrease below the Pyroxenite Marker in the fine-grained gabbro. In the Pyroxenite Marker a minimum barium content was recorded.

In the rocks of Subzone C, the barium values reflected no change, or showed only a minimal increase upwards in the stratigraphical column. The whole-rock values reveal a similar tendency but the values are lower than those recorded for the separated plagioclase feldspar. The barium content of the clinopyroxenes and the orthopyroxenes are all in the region of 5 ppm and are therefore not reflected in Fig. 12. Lateral variation in barium content is slight. The highest values for barium in the normal gabbroic rocks were recorded from the Steelpoortpark borehole.

## 2.2 Chromium

According to Wager and Brown (1968, p.196) chromium enters the early formed pyroxenes and the chromium values therefore decrease rapidly in the magma to a very low concentration in the later differentiates. The reason for this is that  $\text{Cr}^{3+}$  is virtually identical in size with  $\text{Fe}^{3+}$ ,

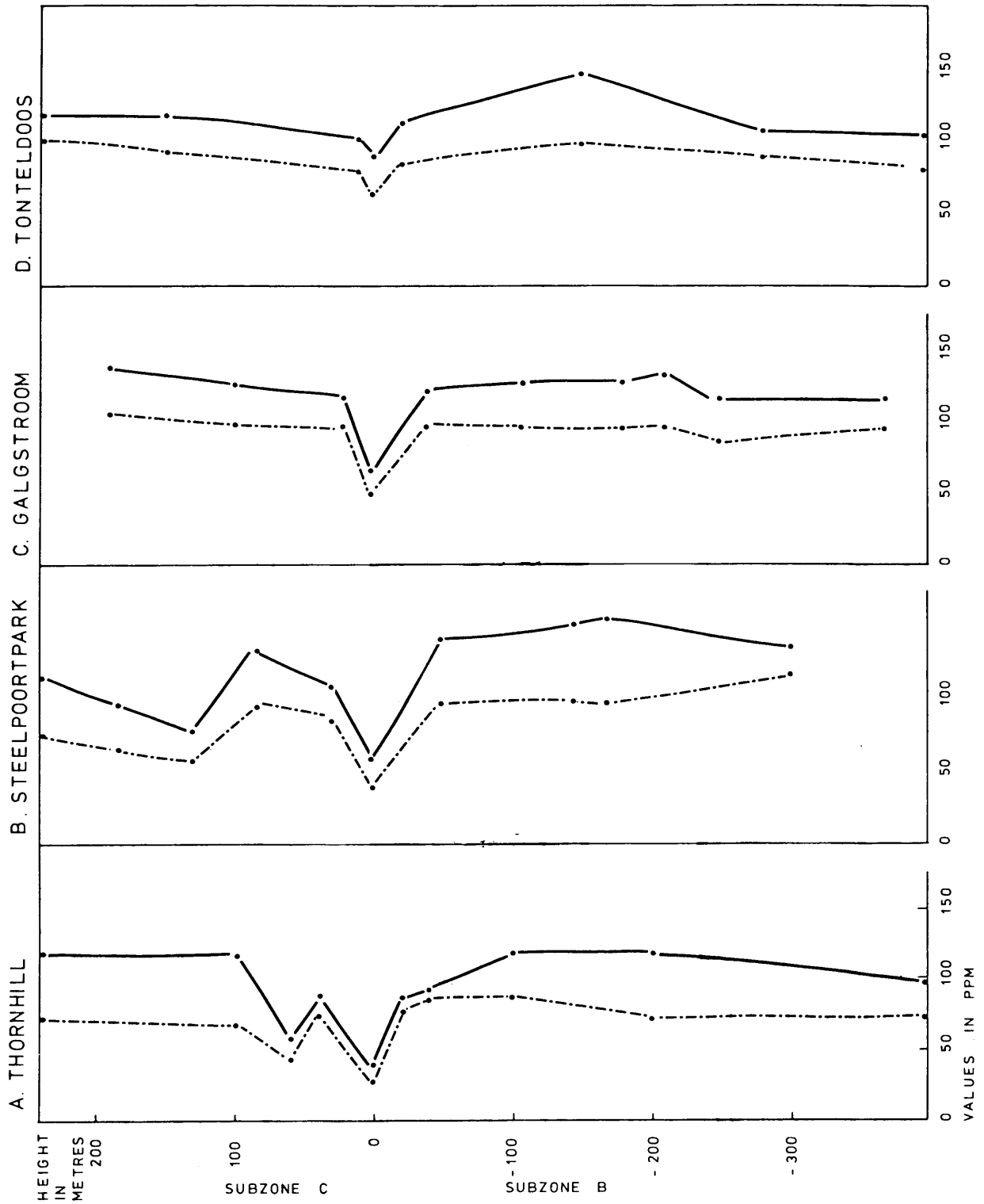


FIG. 12 BARIUM VALUES FOR SEPARATED  
PLAGIOCLASE — AND WHOLE ROCK - - - - -

but forms a more ionic bond with oxygen so that it enters preferentially into  $\text{Fe}^{3+}$  positions. It is consequently depleted at an early stage during the fractional crystallization of a basic magma. Chromium should theoretically be captured in  $\text{Fe}^{2+}$  positions, but charge difficulties restrict this, as is proved by its very limited entry into Skaergaard olivines and ilmenites, compared with its entry into pyroxenes and magnetites (Wager and Mitchell, 1951, p.183). Thus, the absolute concentration of chromium in the rock sequence should be a very useful indicator of the differentiation process undergone by rocks of basic and ultrabasic parentage (Ahrens et al., 1965, p.170).

The chromium content of the analysed rocks and minerals in Subzone B remains constantly low throughout the Subzone in all the areas (Fig. 13). At the stratigraphic height of the Pyroxenite Marker there is a marked increase in the quantity of chromium, and in Subzone C the chromium content is more than twice the amount determined in the rocks below the marker. This trend supported by the fact that chromium, because of its high OSPE, partitions strongly into early magnesium-rich pyroxenes (Burns, 1970, p.148) is a very strong indication that the chromium was introduced by a heave of fresh parent-magma.

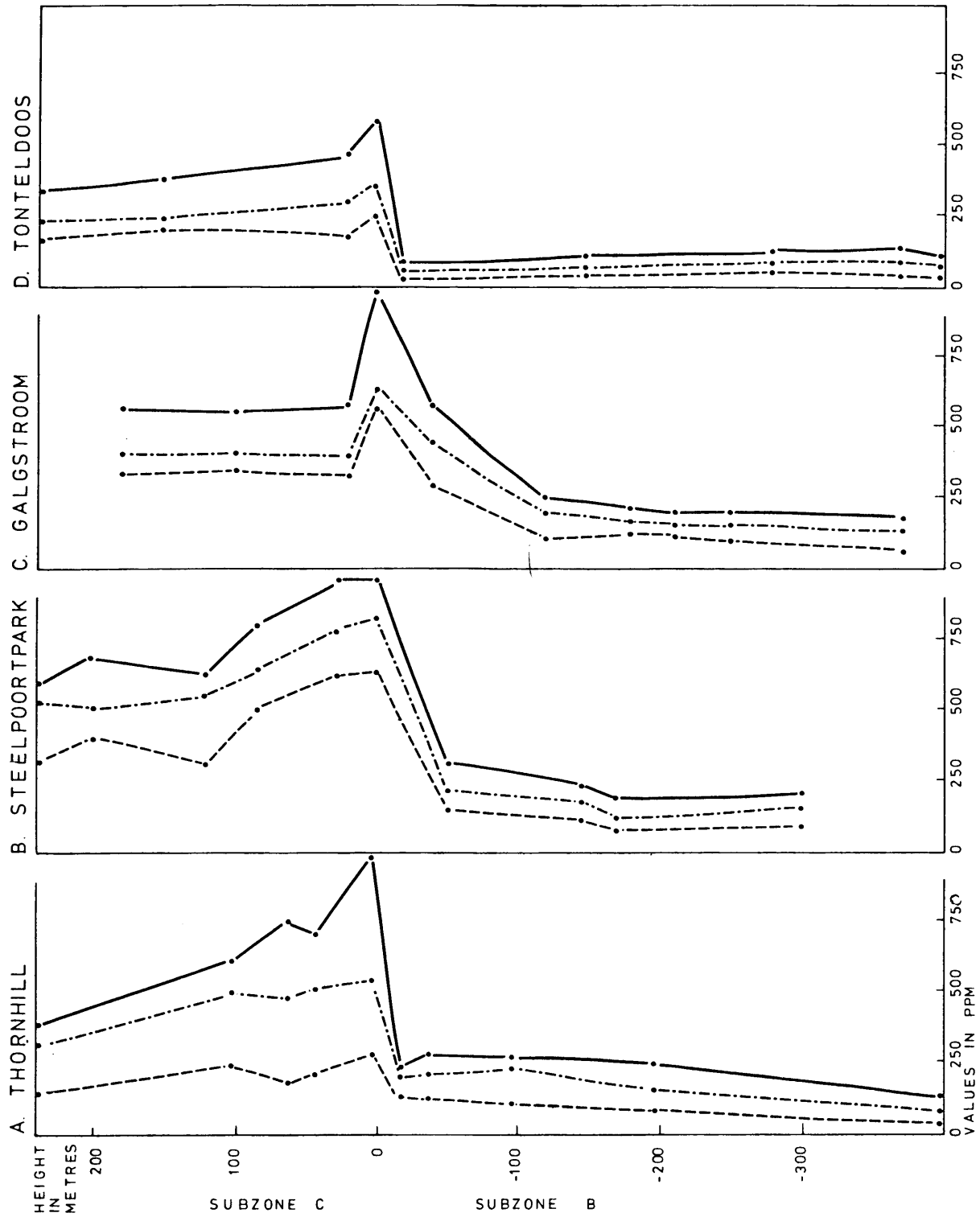


FIG. 13 CHROMIUM VALUES FOR ORTHOPYROXENE.....  
CLINOPYROXENE ——— AND WHOLE ROCK - - - -

### 2.3 Cobalt

Cobalt is normally concentrated in the intermediate stages of fractionation, after which it decreases (Wager and Brown, 1968, p.197). The larger size of the  $\text{Co}^{2+}$  as opposed to the  $\text{Ni}^{2+}$  ion will restrict its entry into magnesium positions to a greater degree than for  $\text{Ni}^{2+}$ , which is otherwise very similar to cobalt. On account of the smaller radius of  $\text{Co}^{2+}$  compared with  $\text{Fe}^{2+}$ , cobalt would substitute for  $\text{Fe}^{2+}$  in the early-formed minerals, but to a lesser extent than  $\text{Ni}^{2+}$ . Because of this, nickel is depleted at a more rapid rate than cobalt in the magma (Ahrens *et al.*, 1965, p.171). Also, according to Burns (1970, p.15) ions which have  $d^2$  and  $d^7$  configurations such as the  $\text{Co}^{2+}$  ion acquire relatively high stabilization energies in tetrahedral co-ordination, whereas the  $\text{Co}^{3+}$  ion is expected to show strong preferences for the octahedral co-ordination sites.

In the basic rocks cobalt prefers to enter olivine where the divalent cations are readily accommodated, because of the absence of difficulties in charge balance. The separated plagioclase rendered values of only approximately 5 ppm and these results were discarded.

In Subzone B (Fig. 14) the cobalt content below the Pyroxenite Marker shows very little change. The more iron-rich rocks of Tonteldoos have an over-all higher content

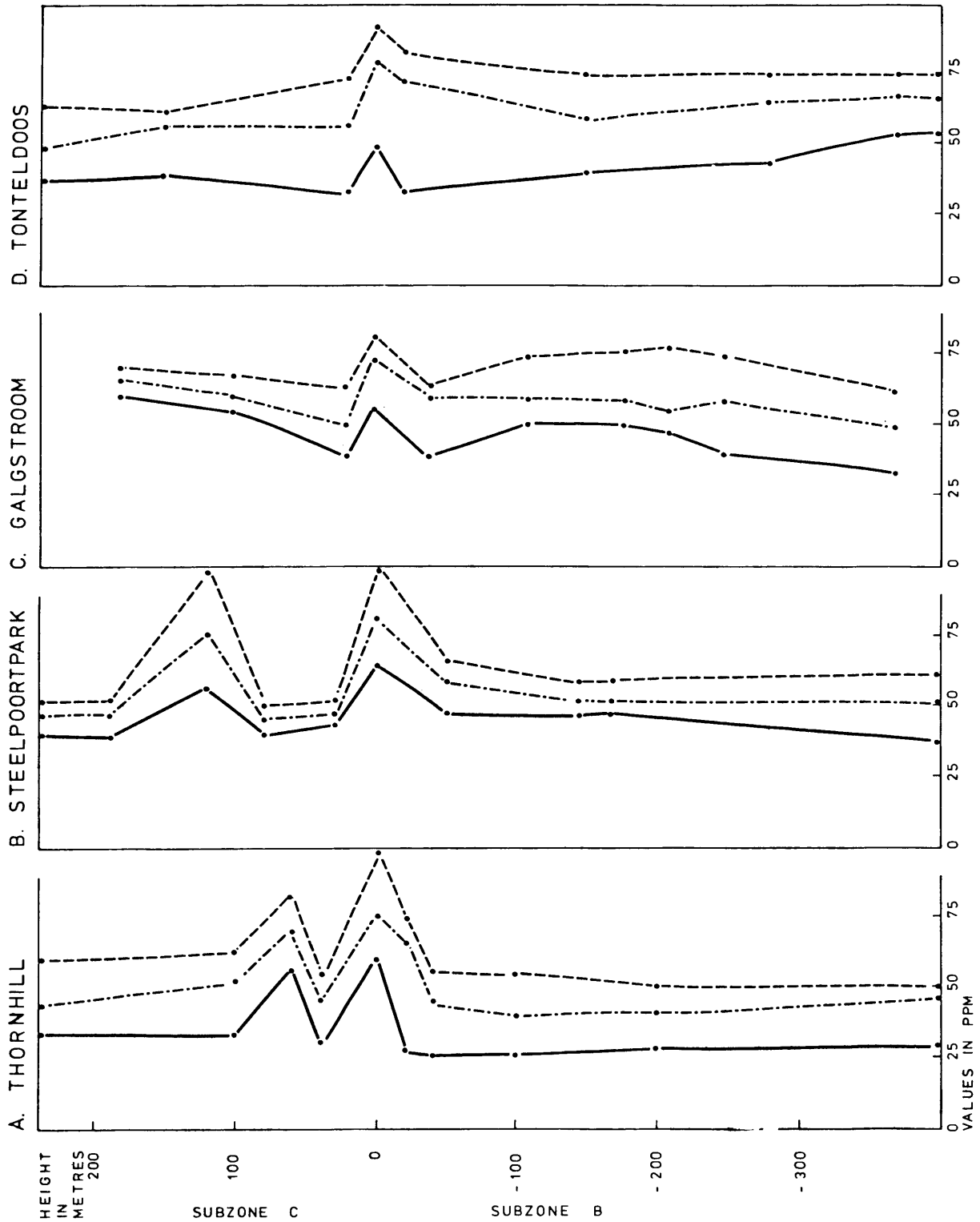


FIG. 14 COBALT VALUES FOR SEPARATED ORTHOPYROXENE.....  
CLINOPYROXENE -.-.-, AND WHOLE ROCK \_\_\_\_\_

of cobalt than the rocks in the north, the only exception being those in the pyroxenites in the northern localities. This increase in cobalt content can be ascribed to the magnesium-rich nature of these rocks.

In Subzone C, the cobalt content shows a tendency to decrease above the Pyroxenite Marker. This could be due to the lower iron content of these rocks compared with those of Subzone B.

#### 2.4 Copper

Among the elements the  $\text{Cu}^+$  ion is similar in size to the  $\text{Na}^+$  ion, whereas the  $\text{Cu}^{2+}$  ion is similar in size to the  $\text{Fe}^{2+}$  ion. In the absence of sulphur, the  $\text{Cu}^+$  ion can enter plagioclase, substituting for  $\text{Na}^+$  and  $\text{Ca}^{2+}$ , and it can also enter minerals containing the  $\text{Fe}^{2+}$  ion. Depending on the initial content of copper in the magma, the concentration will eventually build up until a copper-rich sulphide phase appears in the presence of adequate sulphur (Ahrens, et al., 1965, p.176). Copper also has a low OSPE (Burns, 1970, p.111) and the rate of depletion in the magma would consequently also be low, unless a phase rich in sulphide appears.

The copper content remains very low in all the samples in the succession in the four areas, and is usually well below 40 ppm (Appendix IV). However, in the south at Tonteldoos

an anomalously high copper content is recorded in three specimens of the fine-grained gabbro. The copper content in the samples of whole-rock varies between 400-500 ppm, whereas the copper values are usually higher in the orthopyroxene than in the clinopyroxene (Appendix IV). In polished sections of the fine-grained gabbro, minor amounts of chalcopyrite and bornite were found, together with appreciable amounts of pyrrhotite and magnetite.

## 2.5 Nickel

The enrichment of nickel in minerals like olivine, which usually appears at an early stage during fractional crystallization of magmas is well established (Wager and Mitchell, 1951, p.187). The preference of nickel for the olivine structure, where divalent cations are readily accommodated, can be ascribed to the absence of difficulties to maintain a charge balance (Ahrens et al., 1965, p.173). Nickel also enters the early-formed pyroxenes in the absence of olivine, and further has a preference for the orthopyroxene. Nickel behaves similarly to chromium in that it also reaches a maximum concentration in the early cumulates and decreases in the later-formed rock sequence. Because nickel has a lower OSPE (Burns, 1970, p.160) than chromium, its rate of depletion in the magma is correspondingly lower.

In the rocks of Subzone B, the nickel values vary very little. In the sulphide-bearing magnetite-rich rocks at Tonteldoos (Fig.15D) less than 100 ppm of nickel are present. This implies that very little nickel was present during the separation of the sulphide phase. In view of the strong chalcophile affinities of nickel it would have been extracted from the magma if it had been present in greater quantities.

In Subzone C, from the Pyroxenite Marker upwards, there is an increase in the nickel content. At Tonteldoos in the south the nickel content also increases in this Subzone. This suggests that the nickel was most probably introduced during an influx of fresh magma which gave rise to the Pyroxenite Marker. Laterally, the rocks from the northern areas are richer in nickel than those in the south (Fig. 15)

## 2.6 Strontium

The  $\text{Sr}^{2+}$  ion is intermediate in size between the  $\text{Ca}^{2+}$  ion and the  $\text{K}^+$  ion. It is too large to be camouflaged by the  $\text{Ca}^{2+}$  ion, particularly since the latter ion freely enters sixfold coordination with oxygen. Although the Sr-O bond is more ionic than the Ca-O bond, this effect is overshadowed by the size difference, and strontium enters eightfold coordination positions with oxygen (Ahrens *et al.*, 1965, p.154).

Strontium may be expected to increase relative to Ca during

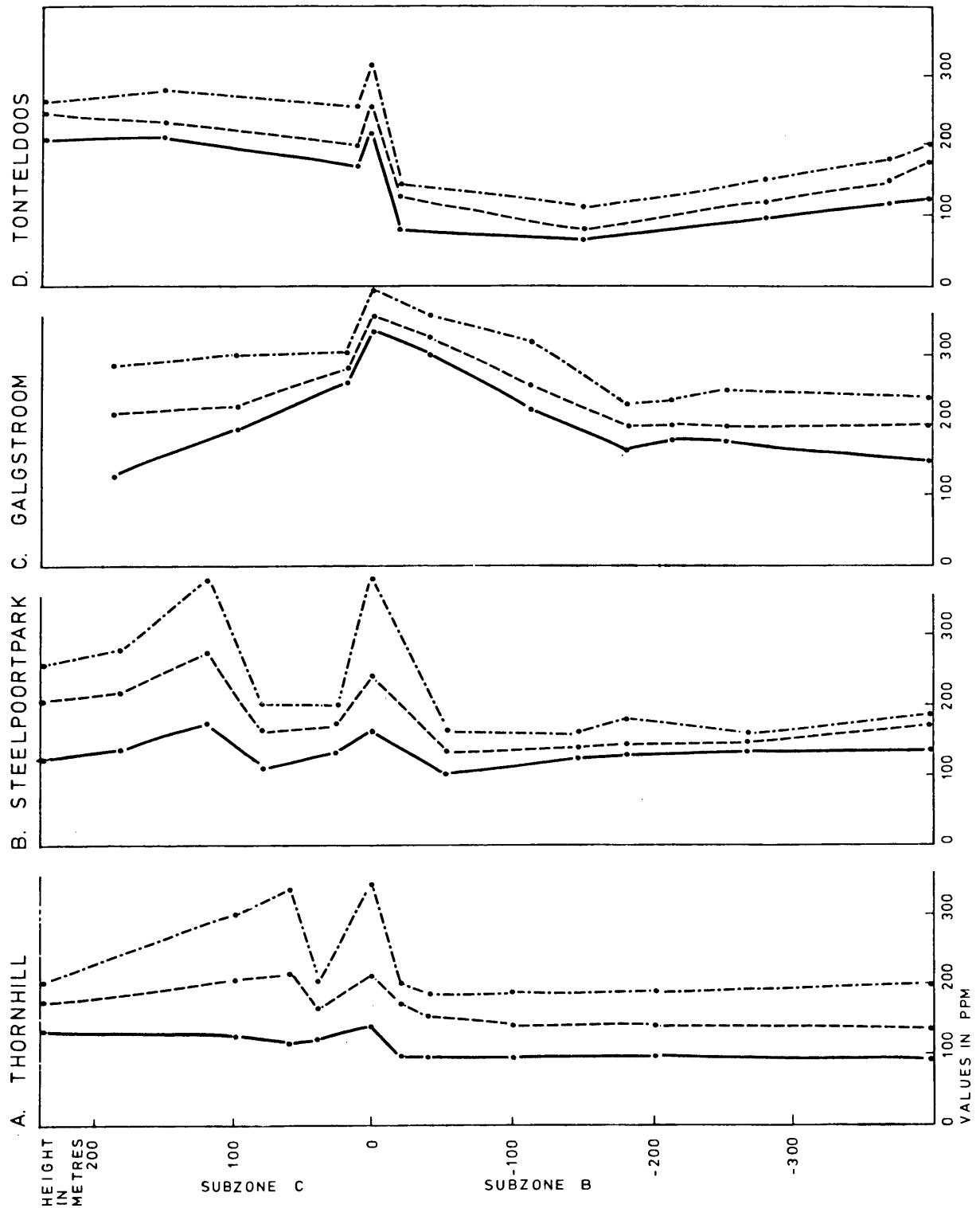


FIG. 15 NICKEL VALUES FOR SEPARATED ORTHOPYROXENE - · - · -  
CLINOPYROXENE - - - AND WHOLE ROCK - - -

fractionation. Strontium enters plagioclase but does not enter the pyroxenes to any marked extent, because, although Ca is surrounded by eight oxygen ions, it is bonded to six only (Wager and Mitchell, 1951).

In Subzone B, the strontium content of the rocks does not vary much (Fig.16). The over-all trend shows higher strontium values than those recorded in Subzone C. At the Pyroxenite Marker a sharp decrease in the strontium content of the plagioclase feldspar as well as of the whole-rock was recorded. Laterally the rocks in the south are richer in strontium than those in the north (Fig. 16).

## 2.7 Vanadium and titanium

Vanadium is present principally as the  $V^{3+}$  ion but the value of the ionic potential is sufficiently high to cause the formation of complexes in the magma. This phenomenon explains the late appearance of vanadium in residual melts (Ahrens et al., 1965, p.168). The  $V^{3+}$  ion forms a more ionic bond than does the  $Fe^{3+}$  ion and this offsets to some extent its larger size. The  $V^{3+}$  ion is very similar to  $Cr^{3+}$  in chemical properties, but the smaller size of the latter ion causes it to enter earlier crystals in greater amounts than the  $V^{3+}$  ion. Also ions with  $d^2$  and  $d^7$  configuration such as the  $V^{3+}$  ion acquire relatively high stabilization energies

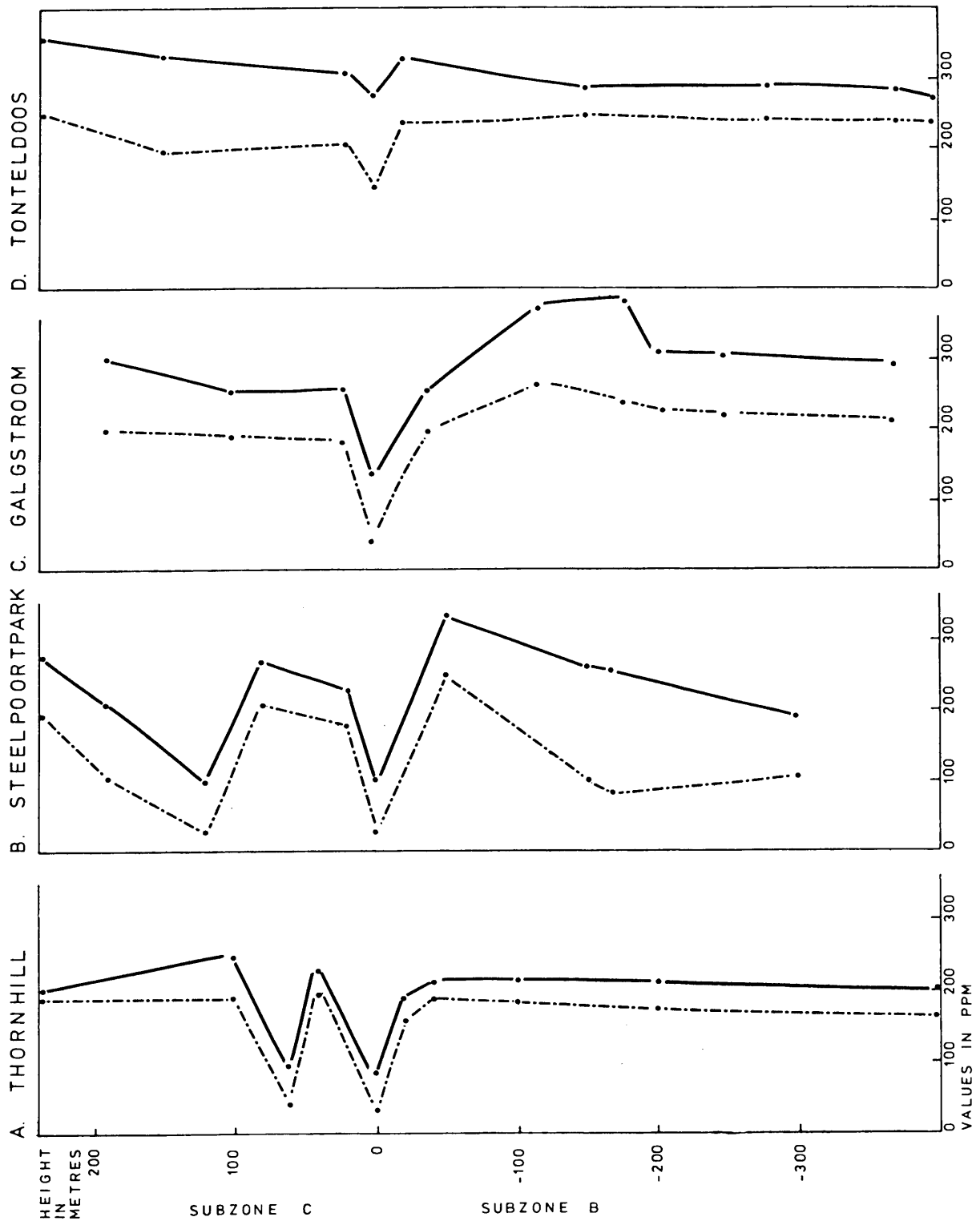


FIG. 16 STRONTIUM VALUES FOR SEPARATED PLAGIOCLASE AND WHOLE ROCK

in tetrahedral coordination (Burns, 1970, p.15). The entry of the  $V^{3+}$  ion into the positions of the  $Fe^{2+}$  ion leads to a difficulty in maintaining the charge balance in minerals such as olivine. In fact, vanadium was not detected at all in olivine from the Skaergaard Complex, but instead is concentrated in the pyroxenes and oxide-minerals (Wager and Mitchell, 1951, p.185). The difficulty in maintaining electrical neutrality in minerals like olivine, leads to the virtual exclusion of the trivalent cations ( $V^{3+}$  and  $Cr^{3+}$ ) although large amounts of  $Ni^{2+}$  and  $Co^{2+}$  enter readily. The reverse situation holds for the pyroxenes (Ahrens et al., 1965, p.168). Because ferric iron is scarce in the early stages of magmatic evolution, much precipitation of vanadium is not to be expected until the main precipitation of ferric iron takes place as the ferrous-ferric oxide (Goldschmidt, 1954, p.489).

Titanium is strongly lithophile. The ionic radius of the  $Ti^{4+}$  ion is 0,64 Å, and it prefers a coordination by six oxygen ions in an approximately octahedral arrangement. Titanium cannot replace silicon in crystalline silicates, because the titanium ion is too large to fit into the tetrahedral coordination by four oxygen ions (Goldschmidt, 1954, p.409).

At Tonteldoos in the fine-grained magnetite-rich rocks of Subzone B, the vanadium content reaches values of

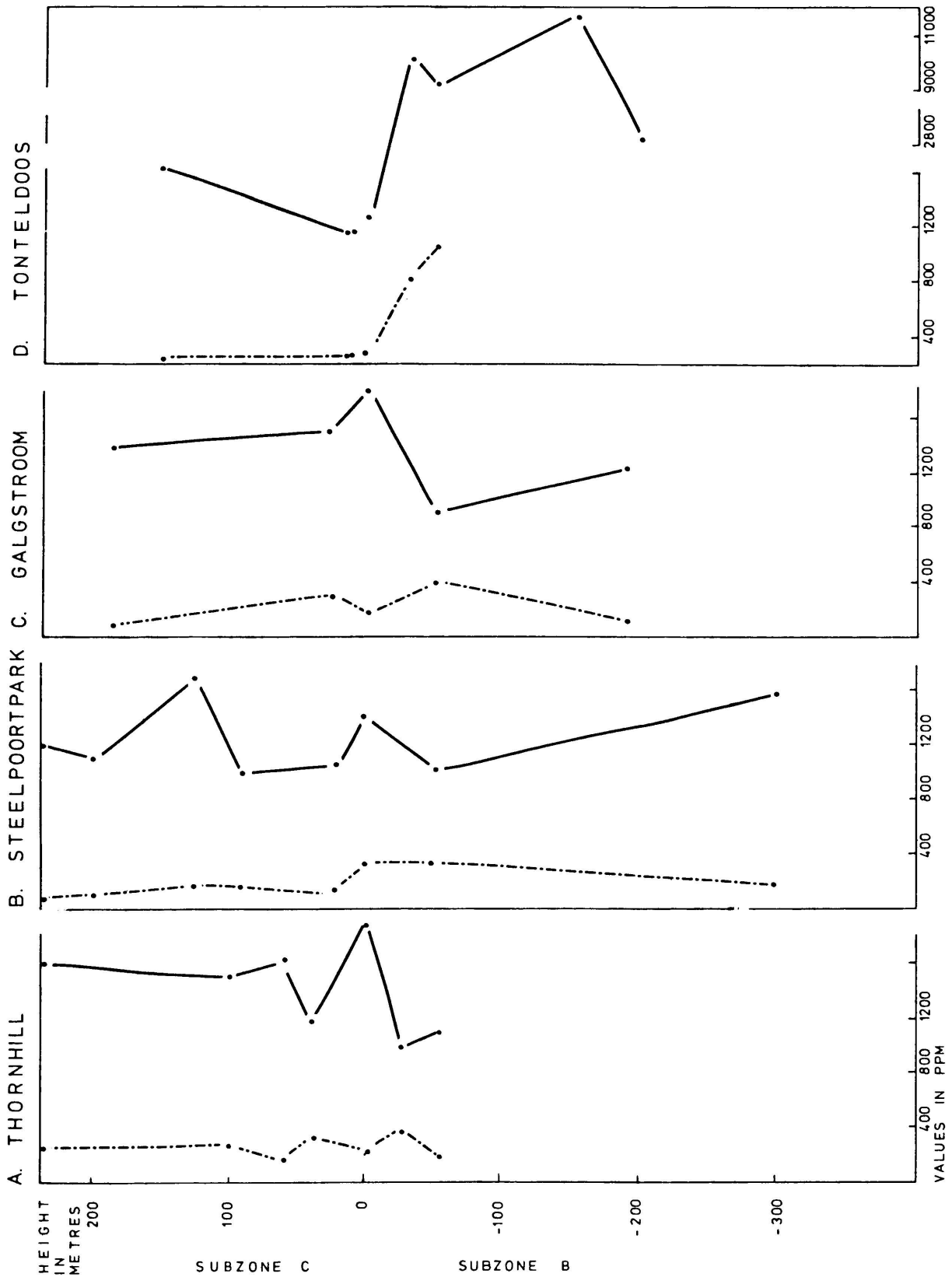


FIG. 17 TITANIUM— AND VANADIUM ..... VALUES WHOLE ROCK.

approximately 880 ppm, while in the correlated horizon at Thornhill 544KS, Steelpoorpark 366KT, Roossenekal and Galgstroom the average vanadium content is 380 ppm, 320 ppm and 395 ppm respectively (Appendix IV). The vanadium content in the rocks from Subzone C remains unchanged.

The titanium content in the fine-grained rocks at Tonteldoos is high and averages about 10 000 ppm (Appendix IV) whereas the values recorded in the rocks from the north are about 1000 ppm throughout the sequence. Where the compositional break takes place in the south, the titanium suddenly decreases to 1200 ppm while in the areas where the pyroxenites are developed, the concentration of titanium increases (Fig.17). A large proportion of the titanium is probably contained in the ferromagnesian silicates, and this is probably the reason for the high titanium values recorded in the pyroxenites. In general the results reflect the inverse relationship which exists between vanadium and titanium.

## 2.8 Zinc

The  $Zn^{2+}$  ion is very nearly the same size as the  $Fe^{2+}$  ion. Although zinc has a zero OSPE, its partitioning behaviour is dominated by its chalcophile affinity (Burns, 1970, p.12). Consequently zinc appears to discriminate

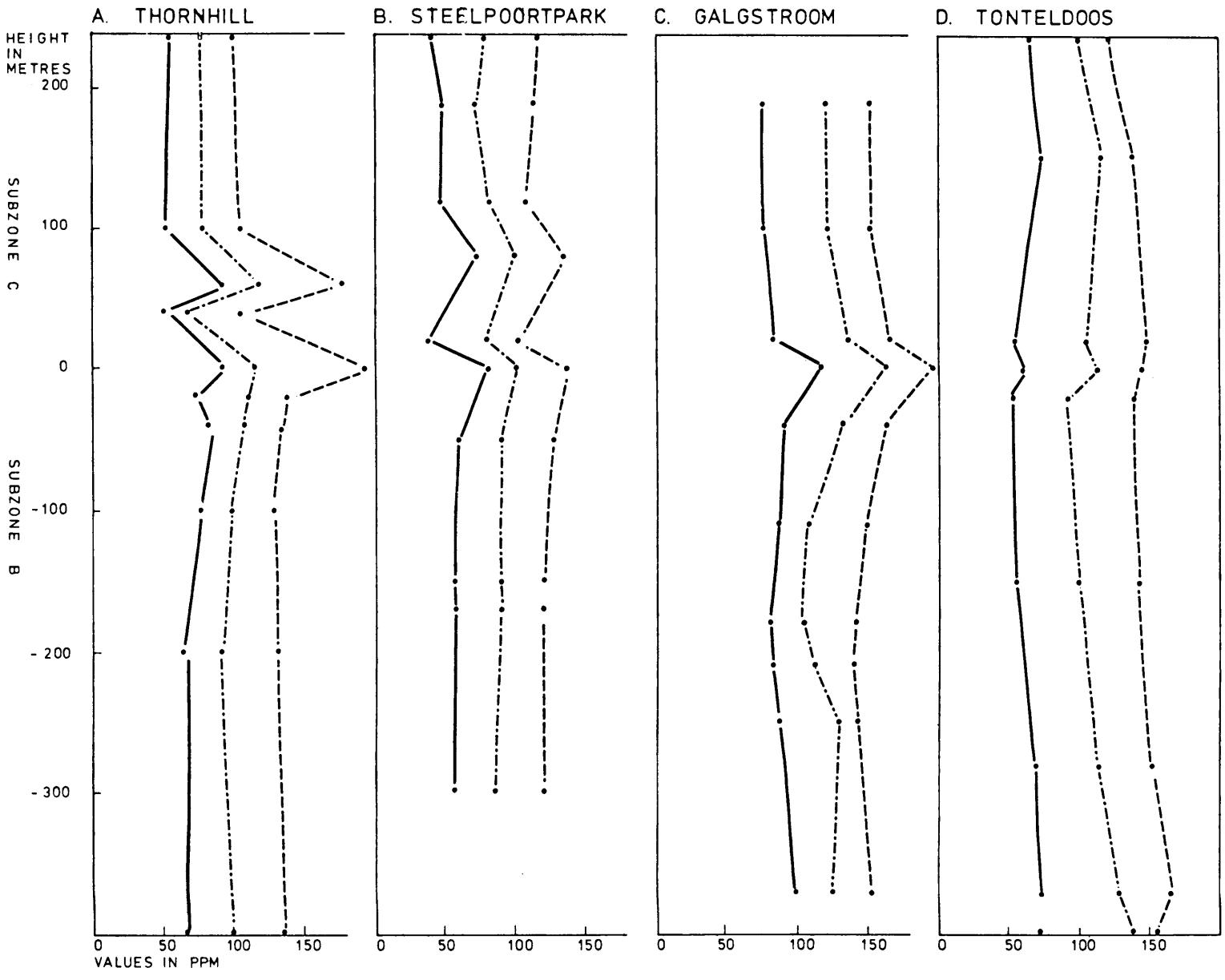


FIG. 18 ZINC VALUES FOR SEPARATED ORTHOPYROXENE - - - - - AND WHOLE ROCK ———

against the octahedral sites in the ferromagnesian silicates and rather forms minerals such as sphalerite (ZnS) (Burns, 1970, p.146).

The over-all fractionation trend for zinc is given in Fig 18. The trend indicates a slightly higher zinc concentration in the rocks of Subzone B, than in the rocks of Subzone C. Laterally the southern areas are richer in zinc than the northern localities, except at the level of the pyroxenite layers, where a marked increase in the zinc is evident in the north. The average zinc concentration of the rocks in the four localities in both subzones is well below 150 ppm.

### 3 Discussion

The main factors controlling the concentration of trace-elements in the magma are the formation of primary precipitate crystals during slow cooling, and the selective action of these on the trace-elements in the magma.

From the diagrams it is clear that when crystals are forming by a process of fractional crystallization they exercise a strong selective action on the trace-elements present in the magma. It is also clear that pyroxenes constitute a suitable host for a greater number of elements analysed than does plagioclase feldspar.

Variations in the chromium and nickel contents with fractionation were shown to be consistent with those predicted by the crystal field theory. Because of its high OSPE, chromium partitions strongly into early magnesium-rich pyroxenes. However, at the Pyroxenite Marker, the reversals of the normal fractionation trend is shown by an increase in chromium content of the pyroxenes from this horizon upwards in the succession. This may represent chromium which was introduced during a new heave of parent magma.

According to Drake and Weill (1975, p.703) fractionation of plagioclase will impoverish the coexisting liquid in strontium and enrich it in barium. If the rocks presently under discussion were products of normal fractional crystallization, then it is to be expected that the barium content would show an over-all increase with stratigraphic height. However, this is not reflected by the values recorded for barium.

The relatively high concentration of copper in the magnetite-rich rocks at Tonteldoos indicates the presence of sulphur at this height of the intrusion, which is in accordance with experimental evidence provided by Haughton et al.(1974). The crystallization of magnetite seems to have resulted in the extraction of sufficient FeO from the magma to cause a decrease in the solubility of sulphur and the accompanying formation of an immiscible sulphide liquid. The lower crystallization

temperatures of the magma at Tonteldoos in the south, would also have the effect of lowering the solubility of sulphur in the magma.

Significant is the fact that very little nickel is present in the sulphide-bearing rocks at Tonteldoos. This implies that very little nickel was present during separation of the sulphide phase. In view of the strong chalcophile affinities of nickel it would have been extracted from the magma, had it been present in large enough quantities at this horizon.

According to Von Gruenewaldt (1976, p.1334) the relatively high nickel content in the copper-rich sulphides of Subzone A and B of the Upper Zone indicates that the Bushveld magma was replenished in nickel at a late stage, and that the addition of fresh, undifferentiated magma at the level of the Pyroxenite Marker in the Main Zone could have been responsible for such an addition of nickel. The trace-element studies of the pyroxenes and whole-rock, within and below the Pyroxenite Marker strongly suggests that such an addition of magma did take place.

## VI SUMMARY AND CONCLUSIONS

The reversal in the fractionation trend, the compositional break and the distribution of trace-elements above and below

the Pyroxenite Marker indicate that the rocks are not the product of continuous normal fractional crystallization within the magma chamber.

The reversal in the crystallization pattern, together with the compositional break indicate a disturbance of the normal trend of fractional crystallization. The gradual onset of the reversal some 300 m below the Pyroxenite Marker indicates that an influx of some magma took place before the crystallization of the Pyroxenite Marker. The more pronounced break at the Pyroxenite Marker is possibly due to a more sudden, forceful injection of a larger quantity of magma, possibly accompanied by an increase in pressure. The continued reversal above the Pyroxenite Marker indicates that gradual additions of magma continued for some time after the formation of the Pyroxenite Marker.

The appearance of magnetite in the fine-grained suite of rocks at Tonteldoos, as well as the gradual enrichment in the less refractory components of the cumulus minerals in a southerly direction is considered to be due to a lateral temperature gradient during crystallization. This temperature gradient is probably the result of the decrease in thickness of the layered sequence in a southerly direction.

The crystallization of sulphides in the south at Tonteldoos was governed by the FeO-content of the melt,

as well as the presence of some sulphur in the melt at this height of the intrusion.

The fact that very little nickel is present in the sulphide-bearing rocks at Tonteldoos, implies that very little nickel was present during the separation of the sulphide phase. The pronounced increase in not only the nickel content but also the chromium content of the ferromagnesian silicates in the Pyroxenite Marker and above indicate that these elements were replenished during the proposed injection of a large quantity of magma immediately prior to crystallization of the Pyroxenite Marker.

The absolute concentration of trace-elements in separated minerals from igneous rocks are useful indicators of the degree of differentiation of the parent-magma. A detailed study of the Rustenburg Layered Suite, by means of petrographic as well as trace-element analyses, may bring to light more reversals in the differentiation trend. It could also give a better insight into the course of the crystallization process of the whole Bushveld Complex.

## VII ACKNOWLEDGEMENTS

For their constant guidance, I wish to express my appreciation to my promoters, Prof. G. Von Gruenewaldt of the Institute for Geological Research on the Bushveld Complex and Dr. C.P.Snyman of the Department of Geology, of the University of Pretoria. I am also indebted to Prof. D.J.L. Visser, head of the Department, for his encouragement.

The laboratory investigations were carried out at the Geological Survey and at the Council for Scientific and Industrial Research. Assistance during the investigations by Drs. C. Frick and R.J. Wattling, as well as Mr. C.H.S.W. Weinert is gratefully acknowledged. Financial aid for this investigation was provided by the C.S.I.R.

The Bantu Affairs Department allowed access to localities within Sekhukhuneland.

Finally I wish to thank all members of the Department of Geology and my husband Pierre Marais who in some way or another contributed towards this thesis.

REFERENCES

- AHRENS, L.H., PRESS, F., RUNCORN, S.K., UREY, H.C. (1965) Physics and Chemistry of the Earth 6. Pergamon Press, London.  
498 p.
- ATKINS, F.B., (1969) Pyroxenes of the Bushveld Intrusion, South Africa. J.Pet., 10 , 222 - 249.
- BARTH, T.F.W., (1962) Theoretical Petrology (Second Edition).  
John Wiley and Sons, Inc., United States of America, 416 p.
- BELT, C.B., (1964) Atomic Absorption Spectrophotometry and the analysis of silicate rocks for Copper and Zinc.  
Econ. Geol., 59 , 240 - 258.
- BUCHANAN, D.L., (1975) The Petrology of the Bushveld Complex Intersected by Boreholes in the Bethal Area.  
Trans. geol. Soc. S. Afr., 78 , 334 - 348
- \_\_\_\_\_ (1976) The Phase Chemistry of the Bushveld Complex in the Bethal Area. PhD. Thesis (unpubl.) Imperial College of Science and Technology, London S.W.7, 141p.

- BURNS, R.G., (1970). Mineralogical applications of crystal field theory. Cambridge University Press, London NW1 224p.
- BURRI, C., PARKER, R.L. and WENK, E., (1967). Die optische Orientierung der Plagiokläse. Birkhäuser Verlag, Basel und Stuttgart, 334p.
- CAMERON, E.N., (1971). Problems of the eastern Bushveld Complex. Fortschr. Mineral., 48, 86 - 108
- DAVIS, B.T. and BOYD, F.R., (1966). The join  $Mg_2Si_2O_6 - CaMgSi_2O_6$  at 30 kilobars pressure and its application to pyroxenes from kimberlites. J. geophys. Res., 71, 3567 - 3576.
- DEER, W.A., HOWIE, R.A. and ZUSSMAN, J., (1968). An introduction to the Rock-Forming minerals. Longmans, London. 528p.
- DRAKE, M.J. and WEILL, D.F., (1975). Partition of Sr, Ba, Ca, Y,  $Eu^{2+}$ ,  $Eu^{3+}$  and other REE between plagioclase feldspar and magmatic liquid : An experimental study. Geochim. et cosmochim. Acta, 39. 689 - 712.
- GOLDSCHMIDT, V.M., (1954). Geochemistry. Oxford Clarendon. 730p.

GROENEVELD, D., (1970). The structural features and the petrography of the Bushveld Complex in the vicinity of Stoffberg, Eastern Transvaal. Geol. Soc. S.Afr., Spec. Publ. 1, 36 - 45.

GRUENEWALDT, G. VON, (1970). On the phase change orthopyroxene-pigeonite and the resulting textures in the Main and Upper Zones of the Bushveld Complex in the Eastern Transvaal. Trans. geol. Soc. S.Afr., Spec. Publ. 1, 67 - 73.

\_\_\_\_\_ (1971). A petrographical and mineralogical investigation of the rocks of the Bushveld Igneous Complex in the Tauteshoogte-Roosenekal area of the Eastern Transvaal.  
D.Sc.Thesis (unpubl.), University of Pretoria, 228p.

\_\_\_\_\_ (1973a). The modified differentiation index and the modified crystallization index as parameters of differentiation in layered intrusions. Trans.geol. Soc.S.Afr., 76, 53 - 61.

\_\_\_\_\_ (1973b). The Main and Upper Zones of the Bushveld Complex in the Roosenekal area, Eastern Transvaal. Trans. geol. Soc. S.Afr., 76 , 207 - 227.

GRUENEWALDT, G. VON, (1976). Sulphides in the Upper Zone of the Eastern Bushveld Complex. Econ. Geol., 71, 1324 - 1336.

\_\_\_\_\_ and WEBER - DIEFENBACH, K., (1977). Coexisting Ca-poor pyroxenes in the Main Zone of the Bushveld Complex. Contr. Mineral. Petrol. (in Press).

HAUGHTON, D.R., ROEDER, P.L. and SKINNER, B.J., (1974). Solubility of sulphur in mafic magmas, Econ. Geol., 69, 451 - 463.

HESS, H.H., (1941). Pyroxenes of common mafic magmas, Part 1 and 2. Amer. Miner., 26, 515 - 594.

HIMMELBERG, G.R. and FORD, A.B., (1976). Pyroxenes of the Dufek Intrusion, Antarctica. J. Pet., 17, Part 2, 219 - 243.

HUGHES, C.J., (1970). Lateral cryptic variation in the Great Dyke of Rhodesia. Geol. Mag., 107, 319 - 325.

IRVINE, T.N. and SMITH, C.H., (1967). Ultramafic and Related Rocks. (Edited by P.J. Wyllie). John Wiley and Sons Inc. New York. 32 - 49.

- JACKSON, E.D., (1970). The cyclic unit in layered intrusions - a comparison of repetitive stratigraphy in the ultramafic parts of the Stillwater, Muskox, Great Dyke and Bushveld complexes. Geol. Soc. S.Afr., Spec. Publ.1, 391 - 424.
- KERR, P.F., (1959). Optical Mineralogy. McGraw-Hill, New York, 442p.
- KIRKBRIGHT, G.F. and SARGENT, M., (1974). Atomic absorption and fluorescence spectroscopy. Academic Press, London. 798p.
- MACDONALD, J.A., (1967). Evolution of the lower Critical Zone, farm Ruighoek, Western Bushveld: J.Pet., 8, 165 - 209.
- MARKGRAAFF, J., (1976). Pyroxenes of the western Bushveld Complex, South Africa. Trans. geol. Soc. Soc.S.Afr., 79, 217 - 224.
- MOLYNEUX, T.G., (1974). A geological investigation of the Bushveld Complex in Sekhukhuneland and part of the Steelpoort valley. Trans. geol. Soc.S.Afr., 77, 329 - 338.
- ROBINSON, J.W., (1966). Atomic absorption spectrometry. Marcel Dekker Inc. New York. 204p.
- RUSS, J.C., (1972). Elemental x-ray analyses of materials.EXAM methods. EDAX laboratory division, EDAX International Incorp., Prairie View, Illinois, United States of America. 89p.

STRELOW, F.W.E., (1963). Separation of titanium from rare earths, berillium, niobium, iron, aluminium, thorium, magnesium and other elements by cation exchange chromatography. Anal. Chem., 35, 1279 - 1282.

\_\_\_\_\_ and VICTOR, A.H., (1975). Accurate determination of vanadium in rocks by ion exchange chromatography-spectrophotometry. Jour. S.Afr.Chem.Inst., 28, 272 - 277.

STRECKEISEN, A., (1976). To each plutonic rock its proper name. Earth Sci. Rev., 12, 1 - 34.

TROGER, W.E., (1959). Optische Bestimmung der gesteinsbildenden Minerale Teil I. Bestimmungstabellen. Schweitzerbart'sche Verlagsbuchhandlung, Stuttgart. 147p.

WAGER, L.R. and MITCHELL, R.L., (1951). The distribution of trace elements during strong fractionation of basic magma - a further study of the Skaergaard Intrusion - East Greenland. Geochim. et cosmoch.Acta, 1, 129 - 208.

\_\_\_\_\_ and BROWN, G.M., (1968). Layered Igneous Rocks. Oliver and Boyd, London. 588p.



## APPENDIX I MODAL ANALYSES - STEELPOORTPARK 366KT

		SUBZONE C											
Sample No	S80	S100	S140	S180	S220	S260	S288	S320	S450	S489	S500	S502	S505
Height(metres)	+250	+245	+230	+220	+208	+200	+187	+170	+150	+126	+123	+122	+121
Modal analyses (vol%)	46,50	47,30	54,00	53,30	57,00	64,60	56,80	52,60	48,70	56,30	38,60	2,50	7,80
Plagioclase	31,20	31,00	27,80	24,70	25,40	18,30	31,80	26,80	26,20	24,60	28,40	71,50	69,60
Orthopyroxene	21,80	21,30	18,20	21,30	16,80	13,30	11,00	17,00	21,70	17,10	31,00	24,40	22,60
Clinopyroxene	0,50	0,40	-	0,50	0,80	3,80	0,40	3,60	3,40	2,00	2,00	0,60	-
Opaque													
Plagioclase: mol%An													
from:													
Extinction angles	67	66	67	67	67	67	67	66	65	65	66	67	66
2V	68	68	68	68	68	66	68	66	65	66	66	67	67
Orthopyroxene mol%Fs													
from:													
2V	29	28	29	29	29	32	31	32	32	32	32	32	32
Name of rock and remarks:	Clinopyroxene norite. Primary hypersthene.	Gabbro-norite. Primary hypersthene.	Plagioclase-bearing pyroxenite. Primary hypersthene.	Plagioclase-bearing pyroxenite. Primary hypersthene.									

## APPENDIX I MODAL ANALYSES - STEELPOORTPARK 366KT

		SUBZONE C										SUBZONE B			
Sample No		S525	S536	S560	S620	S660	S770	S810	S850	S890	S895	S903	S914	S1070	
Height(metres)		+115	+110	+105	+86	+74	+40	+28	+16	+4	+3	0	-3	-50	
Modal analyses(vol%)		63,50	50,60	53,50	62,60	58,00	40,20	62,80	51,60	68,00	32,60	8,10	23,40	66,60	
Plagioclase		18,30	37,00	34,70	25,80	33,20	31,20	22,60	26,90	17,00	51,40	68,50	60,30	13,60	
Orthopyroxene		17,80	11,30	11,80	8,90	8,90	27,40	13,90	18,90	12,60	13,00	22,90	15,00	14,20	
Clinopyroxene		0,40	1,30	-	2,70	-	1,20	0,70	2,60	2,40	3,30	0,50	1,30	5,60	
Opaque															
Plagioclase:mol%An															
from:		66	67	66	66	66	66	67	66	67	65	66	65	60	
Extinction angles		66	66	65	66	67	66	67	67	67	65	65	65	60	
2V														60	
Orthopyroxene:mol%Fs														60	
from:														60	
2V		32	31	33	33	33	33	32	32	32	27	26	27	32	
Name of rock and remarks:		Clinopyroxene norite. Primary hypersthene.	Plagioclase-bearing pyroxenite. Primary hypersthene. (Pyroxenite Marker).	Clinopyroxene norite. Primary hypersthene.	Fine-grained gabbro-norite. Inverted pigeonite.										

## APPENDIX I

## MODAL ANALYSES - STEELPOORTPARK 366KT

	SUBZONE B												
Sample No Height(metres)	S1380 -145	S1456 -169	S1490 -179	S1530 -191	S1570 -203	S1650 -225	S1690 -240	S1730 -252	S1770 -264	S1810 -276	S1850 -289	S1890 -300	S1918 -309
Modal analyses(vol%)													
Plagioclase	68,60	56,50	64,90	65,00	69,00	67,20	69,00	73,60	68,80	70,60	68,00	56,80	70,00
Orthopyroxene	13,70	11,40	15,10	14,80	9,00	12,50	7,30	16,30	7,50	9,40	20,20	12,40	10,30
Clinopyroxene	17,70	31,80	20,00	20,00	21,60	22,40	18,30	18,20	13,70	21,40	22,30	22,40	17,60
Opaque	-	0,20	-	0,20	0,40	-	0,20	0,90	1,20	0,50	0,30	0,60	-
Plagioclase:mol%An from:													
Extinction angles 2V	60 61	61 61	61 61	- -	62 62	62 60	62 62	- -	63 62	62 62	62 62	61 62	61 61
Orthopyroxene:mol%Fs from:													
2V	32	32	36	-	42	42	42	-	42	40	42	40	42
Name of rock and remarks:	Orthopyroxene gabbro. Inverted pigeonite.	Clinopyroxene norite. Inverted pigeonite.	Orthopyroxene gabbro. Inverted pigeonite.	Orthopyroxene gabbro. Inverted pigeonite.	Orthopyroxene gabbro. Inverted pigeonite.	Orthopyroxene gabbro. Inverted pigeonite.							

APPENDIX I MODAL ANALYSES - ROOSSENEKAL + GALGSTROOM

	SUBZONE C								SUBZONE B		
Sample No Height(metres)	G314 +285	G313 +190	G313a +115	G312 +100	G312a +85	G311 +20	G311a +18	G311b 0	G311c -10	G310 -40	G310a -80
Modal analyses(vol%)											
Plagioclase	53,40	46,50	52,40	58,80	62,50	62,30	62,20	14,90	68,30	68,50	60,90
Orthopyroxene	23,40	28,30	26,40	22,30	10,80	15,20	10,90	58,80	28,40	28,50	30,40
Clinopyroxene	23,20	25,20	21,20	18,90	26,70	22,50	26,90	26,30	3,30	8,00	8,70
Opaque	-	-	-	-	-	-	-	-	-	-	-
Plagioclase:mol%An from: Extinction angles 2V	68 69	68 70	- -	68 70	68 69	65 67	66 66	65 66	61 62	61 62	59 61
Orthopyroxene:mol%Fs from: 2V	29	29	-	33	31	32	32	27	32	32	33
Name of rock and remarks:	Clinopyroxene norite. Primary hypersthene.	Clinopyroxene norite. Primary hypersthene.	Clinopyroxene norite. Primary hypersthene.	Clinopyroxene norite. Primary hypersthene.	Orthopyroxene gabbro. Primary hypersthene.	Orthopyroxene gabbro. Primary hypersthene.	Orthopyroxene gabbro. Primary hypersthene.	Plagioclase-bearing pyroxenite. Primary hypersthene. (Pyroxenite Marker).	Fine-grained clinopyroxene norite. Inverted pigeonite.	Fine-grained clinopyroxene norite. Inverted pigeonite.	Fine-grained clinopyroxene norite. Inverted pigeonite.

## APPENDIX I

## MODAL ANALYSES - ROOSSENEKAL + GALGSTROOM

	SUBZONE B									
Sample No Height(metres)	G309 -110	G308 -180	G307 -210	G307a -250	G306 -370	G305 -400	G304 -440	G303 -490	G302 -540	G301 -580
Modal analyses(vol%)										
Plagioclase	63,20	52,30	67,30	59,60	51,00	57,60	58,00	64,50	70,40	68,50
Orthopyroxene	27,70	27,20	22,70	23,40	25,80	28,60	26,90	18,50	12,60	13,30
Clinopyroxene	9,10	19,60	10,00	16,80	23,20	13,80	15,10	17,00	17,00	18,20
Opaque	-	0,90	-	0,20	-	-	-	-	-	-
Plagioclase:mol%An from:										
Extinction angles 2V	59 61	58 60	56 57	56 57	55 56	57 58	61 59	60 59	55 56	55 56
Orthopyroxene:mol%Fs from:										
2V	32	36	44	44	42	42	39	39	39	39
Name of rock and remarks:										
	Fine-grained clinopyroxene norite. Inverted pigeonite.	Clinopyroxene norite. Inverted pigeonite.	Orthopyroxene gabbro. Inverted pigeonite.	Orthopyroxene gabbro. Inverted pigeonite.	Orthopyroxene gabbro. Inverted pigeonite.					

APPENDIX I MODAL ANALYSES - TONTETLDOOS

	SUBZONE C									
Sample No Height(metres)	T700 +280	T701 +240	T702 +210	T703 +200	T704 +190	T705 +150	T706 +110	T707 +50	T708 +20	T709 0
Modal analyses(vol%)										
Plagioclase	65,50	61,60	63,20	64,50	62,70	65,00	61,00	61,00	61,60	46,10
Orthopyroxene	19,20	23,20	23,00	20,80	21,60	14,10	14,50	26,30	24,60	41,00
Clinopyroxene	15,30	15,20	13,80	13,00	14,30	19,80	23,40	12,50	13,80	11,40
Opaque	-	-	-	1,40	1,40	1,10	1,10	0,20	-	1,50
Plagioclase:mol%An from:										
Extinction angles 2V	67 69	67 69	66 69	66 69	65 67	65 67	65 65	65 64	66 67	63 64
Orthopyroxene:mol%Fs from:										60
2V	30	30	30	30	30	32	32	33	36	40
Name of rock and remarks:	Clinopyroxene norite. Primary hypersthene.	Orthopyroxene gabbro. Primary hypersthene.	Orthopyroxene gabbro. Primary hypersthene.	Clinopyroxene norite. Primary hypersthene.	Clinopyroxene norite. Primary hypersthene.	Clinopyroxene norite. Primary hypersthene.				

## APPENDIX I MODAL ANALYSES - TONTELDOOS

	SUBZONE B								
Sample No Height(metres)	T710 -20	T711 -40	T712 -150	T713 -160	T714 -170	T716 -280	T717 -370	T718 -400	T720 -850
Modal analyses(vol%)									
Plagioclase	64,00	66,50	60,40	50,40	49,50	67,80	60,90	61,80	62,70
Orthopyroxene	7,20	4,30	6,20	18,70	19,90	11,20	18,50	18,90	11,40
Clinopyroxene	22,30	26,20	29,20	29,20	29,40	20,40	20,60	19,30	24,50
Opaque	6,50	3,00	4,20	1,70	1,20	0,60	-	-	1,40
Plagioclase:mol%An from:									
Extinction angles 2V	61 62	61 62	62 62	59 59	58 60	60 60	61 61	61 61	61 61
Orthopyroxene:mol%Fs from:									
2V	42	42	42	41	40	44	44	-	-
Name of rock and remarks:									
	Orthopyroxene gabbro. Inverted pigeonite.	Gabbro-norite. Inverted pigeonite.	Gabbro-norite. Inverted pigeonite.	Orthopyroxene gabbro. Inverted pigeonite.					

APPENDIX II CHEMICAL ANALYSES OF ORTHOPYROXENE

Sample No Height(metres)	THORNHILL 544XS				STEELPOORTPARK 366KT			ROOSSENEKAL+GALGSTROOM				TONTELDOOS			
	D600 +240	D606 +40	D608 0	D610 -20	S100 +245	S903 0	S1070 -50	G311 +20	G311b 0	G310 -40	G309 -110	T701 +280	T705 +150	T709 0	T710 -20
SiO <sub>2</sub>	54,64	53,40	54,61	53,19	53,46	53,23	52,40	53,64	53,59	53,24	52,23	51,82	52,82	52,61	52,20
Al <sub>2</sub> O <sub>3</sub>	1,56	1,60	1,89	1,80	1,60	1,89	1,89	1,60	1,80	1,98	1,98	1,59	1,56	1,55	1,50
TiO <sub>2</sub>	0,31	0,29	0,29	0,27	0,29	0,40	0,30	0,29	0,28	0,35	0,27	0,43	0,33	0,63	0,67
MgO	28,89	23,87	24,31	21,13	23,97	24,87	21,10	23,97	24,31	22,31	21,10	23,60	21,68	21,03	17,53
FeO	12,69	17,93	15,02	19,59	17,93	16,05	20,11	17,93	15,32	17,76	20,11	19,49	20,61	22,03	23,64
MnO	0,35	0,33	0,34	0,36	0,33	0,33	0,36	0,33	0,39	0,35	0,36	0,36	0,35	0,32	0,31
Cr <sub>2</sub> O <sub>3</sub>	0,08	0,05	0,21	0,05	0,05	0,18	0,09	0,05	0,18	0,03	0,05	-	-	-	-
CaO	1,57	1,55	2,21	4,13	1,55	2,23	4,10	1,55	2,73	3,96	4,13	1,48	1,46	1,47	4,15
Na <sub>2</sub> O	0,48	0,09	0,62	0,77	0,09	0,37	0,19	0,09	0,59	0,79	0,77	0,80	0,80	0,79	0,91
K <sub>2</sub> O	-	-	-	-	-	-	-	-	-	-	-	-	-	-	-
Total	100,57	99,21	99,50	101,29	99,27	99,55	100,54	99,45	99,19	100,77	101,00	99,57	99,61	100,43	100,91

STRUCTURAL FORMULAE (number of ions on the basis of 6 oxygens )

(Z)	Si	1,943	1,968	1,942	1,953	1,948	1,944	1,942	1,948	1,962	1,948	1,943	1,938	1,938	1,939	1,931
Al	Al	0,057	0,032	0,058	0,047	0,052	0,056	0,058	0,052	0,038	0,052	0,057	0,064	0,062	0,061	0,069
(WXY)	Al	0,008	0,037	0,032	0,030	0,017	0,025	0,024	0,017	0,040	0,033	0,028	0,006	0,006	0,007	0,001
	Ti	0,008	0,008	0,007	0,007	0,008	0,011	0,008	0,008	0,007	0,009	0,007	0,012	0,009	0,017	0,048
	Mg	1,531	1,315	1,345	1,156	1,315	1,359	1,165	1,315	1,327	1,216	1,163	1,309	1,204	1,161	0,981
	Fe	0,377	0,552	0,456	0,601	0,552	0,490	0,623	0,552	0,469	0,543	0,622	0,607	0,642	0,707	0,742
	Mn	0,010	0,010	0,010	0,011	0,010	0,010	0,011	0,010	0,012	0,010	0,011	0,011	0,011	0,010	0,009
	Cr	0,002	0,001	0,006	0,001	0,001	0,005	0,002	0,001	0,005	0,001	0,001	-	-	-	-
	Ca	0,059	0,061	0,086	0,162	0,061	0,087	0,162	0,061	0,107	0,155	0,163	0,059	0,058	0,058	0,167
	Na	0,033	0,006	0,043	0,054	0,006	0,026	0,013	0,006	0,042	0,056	0,055	0,057	0,057	0,056	0,066
K	-	-	-	-	-	-	-	-	0,002	-	0,002	-	-	-	-	
Z		2,000	2,000	2,000	2,000	2,000	2,000	2,000	2,000	2,000	2,000	2,000	2,000	2,000	2,000	2,000
WXY		2,028	1,990	1,985	2,022	1,970	2,013	2,008	1,970	2,009	2,023	2,040	2,061	1,987	2,016	2,014
% Al in (Z)		2,850	1,630	1,900	2,350	2,600	2,800	2,900	2,600	1,900	2,570	2,850	3,200	3,100	3,100	3,450
Atomic per cent	Mg	77,80	68,20	70,80	60,20	68,20	70,18	59,71	68,20	69,70	63,50	59,70	66,29	63,22	60,26	51,90
	Fe	19,20	28,63	24,60	31,30	28,63	25,31	31,94	28,60	24,70	28,40	31,90	30,72	33,72	36,71	39,27
	Ca	3,00	3,17	4,63	8,50	3,17	4,51	8,34	3,20	5,60	8,10	8,40	2,99	3,06	3,03	8,83

Fe as FeO<sub>3</sub>

APPENDIX II CHEMICAL ANALYSES OF CLINOPYROXENE

Sample No Height(metres)	THORNHILL 544KS				STEELPOORTPARK 366KT			ROOSSENEKAL+GALGSTROOM				TONTELDOOS		
	D600a +240	D606a +40	D608a 0	D610a -20	S100a +245	S903a 0	S1070a -50	G311a +20	G311(b)a 0	G310a -40	G309a -110	T701a +280	T705a +150	T710a -20
SiO <sub>2</sub>	51,58	52,45	52,92	52,48	52,45	52,07	51,93	52,48	52,07	52,17	51,38	52,83	51,48	52,87
Al <sub>2</sub> O <sub>3</sub>	2,20	2,20	2,19	2,36	2,24	2,26	2,02	1,94	2,26	1,87	2,28	2,38	2,36	2,31
TiO <sub>2</sub>	0,41	0,41	0,31	0,73	0,34	0,41	0,33	0,45	0,41	0,36	0,48	0,54	0,73	0,97
MgO	18,67	15,73	16,71	15,44	15,61	15,78	14,97	15,41	16,08	15,66	16,20	14,06	14,31	11,87
FeO	7,50	9,90	8,49	10,13	10,73	9,93	11,27	9,69	8,78	9,01	10,83	12,14	13,04	13,91
MnO	0,27	0,27	0,27	0,24	0,26	0,23	0,33	0,24	0,23	0,23	0,27	0,21	0,24	0,33
Cr <sub>2</sub> O <sub>3</sub>	-	-	-	0,01	0,21	0,19	0,07	-	0,19	-	-	-	-	-
CaO	19,85	17,74	18,48	17,42	17,53	19,03	17,94	19,74	18,32	19,76	18,52	18,26	18,18	17,14
Na <sub>2</sub> O	0,53	0,46	0,62	0,67	0,69	0,63	0,48	0,13	0,63	0,18	0,82	0,56	0,67	0,77
K <sub>2</sub> O	-	0,05	0,04	0,01	0,06	0,06	0,06	-	0,06	-	0,06	0,01	0,01	0,03
Total	101,01	99,21	100,03	99,49	100,12	100,59	99,40	100,08	99,03	99,24	100,84	100,99	101,02	100,20

STRUCTURAL FORMULAE ( number of ions on the basis of 6 oxygens )

(Z)	Si	1,948	1,945	1,946	1,942	1,947	1,938	1,940	1,941	1,943	1,935	1,947	1,950	1,932	1,942
	Al	0,052	0,055	0,054	0,058	0,053	0,062	0,060	0,059	0,057	0,065	0,053	0,050	0,068	0,058
(WXY)	Al	0,043	0,041	0,041	0,045	0,045	0,037	0,029	0,026	0,044	0,026	0,046	0,053	0,035	0,044
	Ti	0,011	0,011	0,008	0,020	0,009	0,011	0,009	0,012	0,011	0,010	0,013	0,015	0,020	0,027
	Mg	0,899	0,884	0,915	0,856	0,863	0,875	0,837	0,851	0,894	0,861	0,856	0,773	0,772	0,705
	Fe	0,229	0,308	0,261	0,315	0,333	0,278	0,364	0,288	0,274	0,286	0,336	0,390	0,430	0,436
	Mn	0,008	0,008	0,008	0,007	0,008	0,007	0,010	0,008	0,007	0,007	0,008	0,006	0,007	0,010
	Cr	0,001	0,001	0,007	-	0,006	0,005	0,002	-	0,005	-	-	-	-	-
	Ca	0,778	0,708	0,728	0,694	0,697	0,759	0,722	0,784	0,732	0,781	0,736	0,722	0,723	0,688
	Na	0,037	0,033	0,044	0,018	0,049	0,045	0,035	0,019	0,045	0,012	0,059	0,040	0,048	0,056
	K	0,001	0,002	0,001	0,001	0,002	0,002	0,002	-	0,002	-	0,002	0,001	0,005	0,001
Z		2,000	2,000	2,000	2,000	2,000	2,000	2,000	2,000	2,000	2,000	2,000	2,000	2,000	2,000
WXY		2,007	1,996	2,013	1,956	2,012	2,019	2,010	1,988	2,014	1,983	2,056	2,000	2,040	1,967
% Al in (Z)		2,600	3,250	2,700	2,900	2,650	3,100	3,000	2,950	2,850	3,250	2,650	2,500	3,000	2,900
Atomic per cent	Mg	50,30	46,20	48,10	45,90	45,60	45,80	43,80	43,80	47,10	44,00	45,50	41,00	40,70	37,10
	Fe	11,30	16,30	13,70	16,90	17,60	14,50	18,50	15,80	14,40	16,00	17,10	20,70	22,10	24,40
	Ca	38,40	37,50	38,20	37,20	36,80	39,70	37,70	40,40	38,50	40,00	37,40	38,30	37,20	38,50

Fe<sup>2+</sup> as FeO

APPENDIX III WHOLE ROCK CHEMICAL ANALYSES

	THORNHILL 544KS							STEELPOORTPARK 366KT						
Sample No	D600	D603	D605	D606	D608	D610	D216	S100	S288	S602	S660	S810	S903	S1070
Height(metres)	+240	+100	+60	+40	0	-20	-400	+245	+187	+90	+74	+28	0	-50
SiO <sub>2</sub>	52,37	52,30	49,98	51,34	53,02	52,20	52,28	52,04	53,10	52,40	52,31	52,96	51,79	52,90
TiO <sub>2</sub>	0,21	0,13	0,26	0,20	0,23	0,30	0,15	0,12	0,13	0,42	0,13	0,67	0,23	0,09
Al <sub>2</sub> O <sub>3</sub>	17,38	17,90	6,22	18,60	3,63	17,60	16,79	16,93	16,48	18,50	18,42	17,51	4,64	16,90
FeO	6,92	7,30	13,92	6,82	14,22	7,60	7,33	6,13	6,10	5,80	7,07	6,90	14,39	8,10
MnO	0,17	0,13	0,27	0,14	0,25	0,14	0,18	0,13	0,14	0,15	0,15	0,17	0,26	0,14
MgO	8,46	6,23	19,87	9,04	21,72	8,40	8,62	9,68	9,70	7,17	7,71	7,57	23,14	6,80
CaO	10,90	12,40	8,50	11,39	5,36	11,10	11,62	11,86	10,92	12,05	10,72	11,39	4,85	11,50
Na <sub>2</sub> O	2,38	3,30	0,20	2,04	0,60	2,30	2,49	2,80	2,94	2,51	2,71	2,47	0,20	2,75
K <sub>2</sub> O	0,22	0,20	0,10	0,22	0,07	0,20	0,18	0,22	0,18	0,18	0,31	0,22	0,06	0,46
P <sub>2</sub> O <sub>5</sub>	0,02	0,08	-	-	0,01	0,01	0,01	0,49	0,09	0,09	0,01	0,01	0,40	0,14
Cr <sub>2</sub> O <sub>3</sub>	0,06	0,07	0,17	0,08	0,22	0,02	0,02	0,05	0,07	0,04	0,10	0,11	0,07	0,02
Total	99,09	100,04	99,72	99,87	99,32	99,87	99,67	100,45	99,85	99,31	99,64	99,98	100,03	99,80

C. I. P. W NORM

Qz	0,36	-	-	-	-	0,43	-	-	-	0,46	-	0,58	0,21	1,20	
Or	1,31	1,18	0,59	1,36	0,42	1,18	1,06	1,30	1,06	1,06	1,84	1,31	0,35	2,72	
Ab	20,23	27,91	1,69	20,23	4,20	21,45	21,13	24,68	24,87	27,80	23,03	21,03	1,69	23,26	
An	36,27	33,44	15,78	36,27	7,19	37,11	34,23	32,98	32,24	38,53	37,35	36,47	11,59	32,41	
Di	Wo	7,49	11,36	10,28	7,49	8,36	9,11	9,83	10,44	10,19	5,47	6,68	8,59	4,12	9,90
Di	En	4,56	6,72	6,98	5,36	5,39	5,54	5,91	7,35	7,37	3,95	3,98	5,14	2,85	5,84
Di	Fs	2,51	4,07	2,51	2,51	2,40	2,11	3,40	2,19	2,06	2,98	2,36	2,99	0,93	3,57
Hy	En	16,61	5,38	38,86	16,61	46,77	13,89	12,96	11,38	10,93	12,34	13,46	13,91	54,76	11,09
Hy	Fs	9,16	3,25	13,96	9,16	20,81	6,47	7,46	3,04	3,21	6,79	7,99	8,10	17,93	6,76
Ol	Fo	-	2,39	2,54	-	2,32	-	1,87	1,80	2,50	-	1,30	-	-	-
Ol	Fa	-	1,59	1,01	-	1,14	-	1,19	1,71	1,96	-	0,85	-	-	-
Mt		1,05	2,12	4,04	1,05	1,23	1,91	0,65	1,98	1,97	0,17	0,90	0,58	4,17	2,35
Il		0,40	0,15	0,44	0,40	0,40	0,33	0,29	0,93	0,47	0,80	0,75	1,28	0,44	0,27
Ap		-	0,31	0,64	-	-	0,02	0,02	0,31	0,33	0,21	0,02	0,02	0,95	0,33
Total		99,95	99,87	99,32	100,44	100,63	99,55	100,00	100,09	99,16	100,56	100,51	100,00	99,99	99,70

MDI	36,34	42,74	23,31	36,34	32,08	37,53	37,58	34,59	36,66	36,27	38,58	37,35	23,23	42,01
MCI	44,62	40,86	54,55	44,64	48,29	43,78	44,31	47,25	46,12	44,66	43,44	43,71	53,80	40,64

Fe as FeO

APPENDIX III (continued)

Sample No Height(metres)	ROOSSENEKAL + GALGSTROOM							TONTELDOOS						
	G311 +20	G311b 0	G310 -40	G309 -110	G308 -180	G307 -210	G301 -580	T701 +280	T705 +150	T708 +20	T709 0	T710 -20	T712 -150	T714 -170
SiO <sub>2</sub>	52,96	53,48	51,18	53,91	55,33	53,66	54,63	52,30	54,89	53,90	51,79	51,30	52,20	50,86
TiO <sub>2</sub>	0,07	0,30	0,10	0,12	0,09	0,14	0,15	0,17	0,19	0,12	0,11	0,30	0,80	0,43
Al <sub>2</sub> O <sub>3</sub>	18,99	4,17	18,78	18,18	18,44	18,13	17,83	19,56	16,98	16,94	14,91	16,99	16,00	14,60
FeO	7,19	13,19	8,80	7,76	7,94	8,61	7,45	6,10	5,10	7,80	12,25	10,80	9,30	12,17
MnO	0,15	0,32	0,15	0,13	0,15	0,15	0,14	0,11	0,11	0,15	0,21	0,14	0,13	0,17
MgO	7,17	22,62	6,61	4,26	3,56	3,68	3,76	6,10	6,98	6,63	7,20	6,35	7,10	8,00
CaO	9,76	4,79	10,88	11,91	11,37	11,62	11,01	12,90	12,01	11,40	10,40	10,92	10,40	11,00
Na <sub>2</sub> O	3,03	0,40	3,81	2,92	3,59	4,30	3,82	2,70	3,40	3,70	2,85	3,25	3,90	2,40
K <sub>2</sub> O	0,22	0,12	0,19	0,23	0,22	0,41	0,45	0,27	0,36	0,22	0,19	0,25	0,28	0,24
P <sub>2</sub> O <sub>5</sub>	0,01	0,03	0,03	0,07	0,15	0,11	0,15	0,08	0,07	0,10	0,11	0,18	0,10	0,13
Cr <sub>2</sub> O <sub>5</sub>	0,03	0,11	0,05	0,02	0,02	0,01	0,02	0,01	0,01	0,04	0,07	-	0,01	0,03
Total	99,88	99,53	100,58	99,51	100,86	100,82	99,41	100,30	100,10	101,00	100,09	100,48	100,22	100,03

C.I.P.W NORM

Qz	-	2,05	-	0,85	-	0,24	2,63	-	1,19	-	-	-	-	-
Or	1,31	0,71	1,12	1,36	1,30	2,42	2,66	1,60	2,13	1,30	1,12	1,48	1,65	1,42
Ab	25,90	3,38	32,22	28,70	32,36	36,37	32,31	22,84	28,76	31,29	27,10	27,49	32,98	20,30
An	37,96	9,23	28,13	35,82	34,56	28,96	30,18	42,19	30,01	28,97	29,33	31,04	25,33	28,36
Di	Wo	4,55	5,98	10,38	9,35	9,13	8,42	8,38	12,04	11,10	9,55	9,27	10,61	10,48
Di	En	2,73	4,19	5,10	4,71	4,72	4,35	5,21	8,09	6,57	5,42	4,82	6,05	5,67
	Fs	1,59	1,29	5,08	4,44	4,82	4,03	2,68	3,04	3,98	3,73	4,20	4,09	4,45
Hy	En	15,19	52,12	5,94	5,90	5,64	5,82	9,83	9,29	7,34	10,60	9,36	7,62	12,75
	Fs	8,83	16,01	5,92	5,56	5,29	7,01	5,06	3,49	4,45	6,31	8,83	4,42	10,02
Ol	Fo	0,09	-	1,70	-	-	-	0,10	-	1,82	1,83	-	1,71	1,05
	Fa	0,06	-	1,87	-	-	-	0,06	-	1,21	1,67	-	1,75	0,91
Mt		1,64	3,82	2,55	2,25	2,30	2,30	1,77	1,48	2,26	3,55	3,13	2,70	3,53
Il		0,13	0,57	0,06	0,13	0,28	0,21	0,15	0,13	0,19	0,21	0,34	0,19	0,25
Ap		0,02	0,07	0,36	0,31	0,36	0,36	0,26	0,26	0,36	0,50	0,33	0,31	0,40
Total		100,00	99,42	100,43	99,38	100,76	100,69	100,13	99,91	100,84	100,92	100,29	99,41	99,59

MDI	39,81	25,87	52,09	46,35	51,64	56,08	53,22	34,96	42,11	46,66	47,09	47,16	43,94	43,00
MCI	42,22	51,95	24,12	37,60	33,89	30,78	32,78	45,61	40,57	37,94	37,29	38,12	39,81	40,28

Fe as FeO

## APPENDIX IV

## TRACE ELEMENT ANALYSES ON SEPARATED MINERALS AND WHOLE ROCK - THORNHILL 544KS

	SUBZONE C					SUBZONE B				
Sample No Height(metres)	D600 +240	D603 +100	D605 +60	D606 +40	D608 0	D609 -20	D610 -40	D611 -100	D613 -200	D216 -400
<u>Barium</u>										
Plagioclase	120	120	60	90	40	87	87	120	120	100
Whole rock	70	70	45	80	30	80	90	90	75	75
<u>Chromium</u>										
Orthopyroxene	301	516	497	506	541	212	248	230	150	74
Whole rock	141	238	213	179	273	125	124	100	95	37
Clinopyroxene	375	600	750	700	1025	225	275	250	250	125
<u>Cobalt</u>										
Whole rock	33	33	57	31	60	27	25	25	29	29
Orthopyroxene	60	63	83	54	95	55	55	55	50	50
Clinopyroxene	43	55	70	45	75	67	45	40	40	45
<u>Copper</u>										
Clinopyroxene	19	14	10	6	15	8	8	7	6	8
Orthopyroxene	27	37	26	26	9	11	11	12	12	9
Whole rock	30	30	17	8	9	9	7	8	8	8
<u>Nickel</u>										
Whole rock	138	130	122	143	143	109	110	100	100	98
Orthopyroxene	205	300	331	205	350	200	180	180	190	200
Clinopyroxene	172	211	220	163	210	160	157	150	148	130
<u>Strontium</u>										
Plagioclase	220	260	100	250	100	200	220	220	230	210
Whole rock	200	200	43	224	43	171	200	180	180	175
<u>Titanium</u>										
Whole rock	1590	1478	1615	1190	1870	985	1110	1000	1000	-
<u>Vanadium</u>										
Whole rock	260	240	165	290	240	380	210	200	220	-
<u>Zinc</u>										
Whole rock	59	59	94	56	90	74	64	80	64	64
Orthopyroxene	100	106	184	110	197	140	139	127	130	138
Clinopyroxene	80	80	112	70	120	110	50	100	90	100

APPENDIX IV TRACE ELEMENT ANALYSES ON SEPARATED MINERALS AND WHOLE ROCK - STEELPOORTPARK 366KT

	SUBZONE C						SUBZONE B			
Sample No	S100	S288	S505	S620	S810	S903	S1070	S1380	S1456	S1890
Height(metres)	+245	+187	+121	+86	+28	0	-50	-145	-169	-300
<u>Barium</u>										
Plagioclase	120	102	80	140	114	60	148	158	160	140
Whole-rock	80	70	60	100	90	40	100	100	100	120
<u>Chromium</u>										
Orthopyroxene	520	500	536	650	775	825	200	180	100	158
Whole rock	304	390	304	510	654	630	140	100	75	75
Clinopyroxene	578	680	625	800	968	954	300	220	180	189
<u>Cobalt</u>										
Whole rock	38	38	55	33	41	65	46	45	46	35
Orthopyroxene	50	50	100	48	50	100	65	57	58	60
Clinopyroxene	46	45	76	45	45	80	58	50	56	50
<u>Copper</u>										
Clinopyroxene	3	4	3	10	11	8	10	9	10	11
Orthopyroxene	10	8	16	13	29	10	14	13	18	21
Whole-rock	21	22	21	17	17	17	20	21	22	26
<u>Nickel</u>										
Whole rock	123	132	177	110	130	162	110	130	130	130
Orthopyroxene	250	273	378	200	200	378	162	188	188	187
Clinopyroxene	201	208	273	150	173	229	142	142	140	157
<u>Strontium</u>										
Plagioclase	284	214	80	269	229	100	325	275	250	190
Whole-rock	200	125	36	214	188	34	250	100	80	108
<u>Titanium</u>										
Whole-rock	1205	1105	1680	990	1055	1415	1415	1440	1388	1550
<u>Vanadium</u>										
Whole-rock	120	120	180	150	135	320	320	259	243	180
<u>Zinc</u>										
Whole rock	39	49	47	72	47	80	60	57	60	57
Orthopyroxene	119	115	108	137	102	135	120	120	118	118
Clinopyroxene	80	70	81	100	80	100	90	90	90	82

## APPENDIX IV TRACE ELEMENT ANALYSES ON SEPARATED MINERALS AND WHOLE ROCK - ROOSSENEKAL + GALGSTROOM

SUBZONE C					SUBZONE B					
Sample No	G313	G312	G311	G311b	G310	G309	G308	G307	G307a	G306
Height(metres)	+190	+100	+20	0	-40	-110	-180	210	-250	-370
<u>Barium</u>										
Plagioclase	140	130	120	66	126	130	130	138	120	120
Whole-rock	110	100	100	50	100	100	100	100	90	108
<u>Chromium</u>										
Orthopyroxene	400	402	400	625	459	200	175	150	145	150
Whole rock	335	343	340	580	300	109	130	100	100	50
Clinopyroxene	560	556	566	1080	570	230	200	192	200	175
<u>Cobalt</u>										
Whole rock	60	55	39	55	40	50	50	48	40	34
Orthopyroxene	70	68	64	81	64	74	78	78	75	62
Clinopyroxene	65	60	50	75	60	58	59	55	60	50
<u>Copper</u>										
Clinopyroxene	12	11	9	5	5	9	9	9	12	9
Orthopyroxene	19	19	19	19	11	10	11	8	11	11
Whole-rock	16	26	17	30	22	8	7	11	10	8
<u>Nickel</u>										
Whole rock	142	200	262	340	300	228	163	184	160	154
Orthopyroxene	285	290	312	400	362	300	236	238	240	230
Clinopyroxene	224	234	276	364	330	253	180	200	200	210
<u>Strontium</u>										
Plagioclase	298	240	240	150	256	375	390	315	315	300
Whole-rock	200	198	186	43	200	271	228	200	220	214
<u>Titanium</u>										
Whole-rock	1380	1530	1820	930	1070	1250	-	-	-	-
<u>Vanadium</u>										
Whole-rock	150	305	180	395	240	135	-	-	-	-
<u>Zinc</u>										
Whole rock	75	79	83	127	91	90	80	83	90	100
Orthopyroxene	150	155	165	196	161	150	135	140	141	153
Clinopyroxene	120	121	139	160	130	110	110	120	130	126

APPENDIX IV TRACE ELEMENT ANALYSES ON SEPARATED MINERALS AND WHOLE ROCK - TONTELDOOS

	SUBZONE C				SUBZONE B					
Sample No	T701	T705	T708	T709	T710	T712	T716	T717	T718	T720
Height(metres)	+240	+150	+20	0	-20	-150	-280	-370	-400	-850
<u>Barium</u>										
Plagioclase	120	120	106	90	114	150	110	110	106	100
Whole-rock	105	95	80	65	85	100	89	91	80	115
<u>Chromium</u>										
Orthopyroxene	225	225	300	350	75	75	88	100	73	97
Whole rock	168	200	175	250	48	40	50	49	42	54
Clinopyroxene	348	376	470	574	78	100	132	143	100	104
<u>Cobalt</u>										
Whole rock	38	40	34	49	34	40	44	54	53	38
Orthopyroxene	64	62	75	92	86	75	75	75	75	66
Clinopyroxene	50	58	57	80	73	59	65	68	63	65
<u>Copper</u>										
Clinopyroxene	8	10	6	6	404	338	11	11	12	12
Orthopyroxene	14	20	16	12	670	548	22	23	17	16
Whole-rock	8	12	17	8	475	453	11	13	16	17
<u>Nickel</u>										
Whole rock	204	218	174	216	78	82	100	126	135	204
Orthopyroxene	260	270	260	302	195	144	175	175	200	272
Clinopyroxene	250	230	200	253	93	94	125	150	175	226
<u>Strontium</u>										
Plagioclase	365	343	316	283	330	290	286	275	273	269
Whole-rock	257	200	214	157	243	257	251	256	250	243
<u>Titanium</u>										
Whole-rock	-	1620	1170	1250	10340	11720	2865	-	-	-
<u>Vanadium</u>										
Whole-rock	-	245	220	266	880	920	340	-	-	-
<u>Zinc</u>										
Whole rock	65	76	55	55	56	59	68	69	70	73
Orthopyroxene	121	137	154	149	142	142	154	165	155	179
Clinopyroxene	100	135	107	110	90	101	113	130	140	72